



Cite this: *J. Mater. Chem. C*,  
2024, 12, 11265

## Dry ionic conductive elastomers based on polymeric deep eutectic solvents for bioelectronics

Matías L. Picchio, <sup>ab</sup> Antonio Dominguez-Alfaro, <sup>c</sup> Roque J. Minari, <sup>b</sup> Josué D. Mota-Morales <sup>d</sup> and David Mecerreyres <sup>ae</sup>

Polymerizable deep eutectic solvents (PDESs), also known as deep eutectic monomers, have emerged as a versatile material platform for fabricating dry ionic conductive elastomers (ICEs). ICE materials present numerous opportunities for wearable sensors, bioelectrodes, and biomedical device integration. Recent advances have been pursued to expand the current PDES library, incorporating innovative building blocks with multifunctional properties and allowing new families of ionic polymers known as polyDES. In this review, we delve into the central features of PDES, highlighting its macromolecular engineering for tuning its properties and designing new ionic conductive elastomers based on polyDES, including copolymers, dynamic and double networks, or nanocomposites. In addition, additive manufacturing techniques for structuring these ionic polymers are also overviewed. Finally, the latest advances in their bioelectronic applications, as well as current demands and potential opportunities for future developments of PDES, are discussed.

Received 27th April 2024,  
Accepted 2nd July 2024

DOI: 10.1039/d4tc01732c

[rsc.li/materials-c](http://rsc.li/materials-c)

<sup>a</sup> POLYMAT University of the Basque Country UPV/EHU, Paseo Manuel de Lardizábal, 3, 20018 Donostia-San Sebastián, Spain.

E-mail: matias.picchio@polymat.eu

<sup>b</sup> Instituto de Desarrollo Tecnológico para la Industria Química (INTEC), CONICET, Güemes 3450, Santa Fe 3000, Argentina

<sup>c</sup> Electrical Engineering Division, Department of Engineering, University of Cambridge, 9 JJ Thomson Ave, Cambridge, UK

<sup>d</sup> Centro de Física Aplicada y Tecnología Avanzada, Universidad Nacional Autónoma de México, Querétaro, Querétaro 76230, Mexico

<sup>e</sup> IKERBASQUE, Basque Foundation for Science, Plaza Euskadi 5, 48009 Bilbao, Spain

## 1. Introduction

Bioelectronics is a rapidly evolving multidisciplinary domain that integrates biology and microelectronics for diagnostic and therapeutic applications in modern healthcare.<sup>1,2</sup> Typical applications include wearable sensors for monitoring temperature, pressure, motion, and physiological activity,<sup>3,4</sup> brain-machine interfaces,<sup>5,6</sup> and biodegradable implantable devices that stimulate healing (Scheme 1).<sup>7,8</sup> However, the interface between



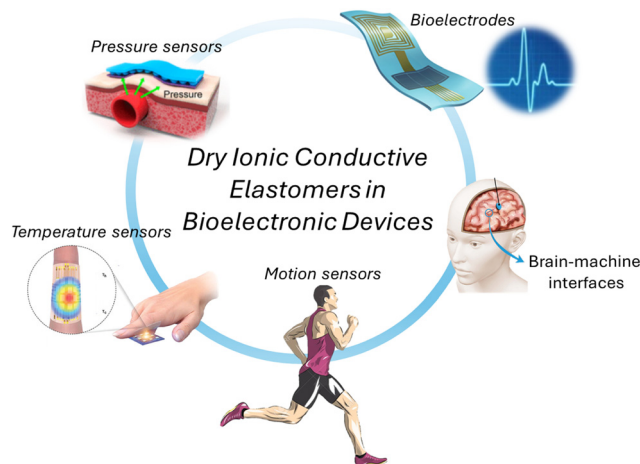
Matías L. Picchio

Matías L. Picchio is a postdoctoral researcher at POLYMAT-University of the Basque Country (San Sebastián, Spain). He received his PhD in 2016 from the National University of the Litoral (Santa Fe, Argentina) and joined POLYMAT in 2022 as a Marie Skłodowska-Curie fellow. His research interests include developing and applying functional soft materials in the biomedical space. He is a passionate amateur chess player and pet lover, aspiring to become a future research leader in eutectic-based materials.



David Mecerreyres

David Mecerreyres is an Ikerbasque Research Professor at POLYMAT, University of the Basque Country in Spain. His current research interests include the design of new polymers for applications in emerging technologies in energy, as well as bioelectronics. He has published over 400 peer-reviewed articles. He is an associate editor of the ACS Applied Polymer Materials journal and a member of the Advisory Board of Materials Horizons.



**Scheme 1** Schematic illustration summarizing different applications for ionic conductive elastomers as wearable sensors and bioelectrodes in bioelectronics.

biological tissues and electronic systems is challenging due to the inherent mismatch in mechanical properties (soft *vs.* rigid) and electrical communication (ionic *vs.* electronic signals).<sup>9</sup> Recent advances in materials design have allowed the development of flexible and stretchable conductors to bridge this gap, enabling compliant electrode coupling to biological systems.<sup>10</sup> Therefore, soft materials have played a pivotal role in the past decade, broadening the scope of bioelectronics and showing great promise for revolutionizing healthcare.<sup>11</sup>

Polymeric hydrogels are perhaps the most popular soft conductors intensively used in bioelectronics, which can be engineered at the molecular level to exhibit precise control over their mechanical, ionic, electrical, and biochemical features.<sup>12–14</sup> Furthermore, their water-rich nature and biocompatibility minimize adverse reactions when interfaced with biological systems.<sup>15,16</sup> Conductive polymers,<sup>17,18</sup> such as poly(3,4-ethylenedioxythiophene) (PEDOT),<sup>19</sup> polyaniline (PANI),<sup>20</sup> polypyrrole (PPy),<sup>21</sup> and polythiophene,<sup>22</sup> or inorganic conductive additives,<sup>23</sup> including carbon nanotubes (CNTs), graphene, metal nanowires, liquid metal droplets,<sup>24</sup> and 2D transition metal carbides/nitrides (MXenes)<sup>25</sup> are commonly incorporated into the hydrogel matrix to construct flexible electronics. Although they have several benefits, hydrogels fail in long-term recording in bioelectronic applications as they dehydrate when exposed to the open air.<sup>26,27</sup> Besides, water freezing at sub-zero temperatures in hydrogels limits their operation range.<sup>28</sup>

In the last few years, ionogels made of ionic liquids with very low vapor pressure have been proposed to overcome these drawbacks of hydrogels, and they have been investigated in several applications, including devices for electrophysiology,<sup>29,30</sup> artificial skin,<sup>31–33</sup> sensors,<sup>34,35</sup> and organic transistors.<sup>36,37</sup> Several review articles addressing ionogels for bioelectronics have been recently published for interested readers.<sup>38–40</sup>

As the bioelectronic field is continuously seeking innovative soft conducting materials, the emergence of deep eutectic solvents (DESs) as novel green electrolytes has recently moved

the focus from ionogels to eutectogels and dry elastomers based on polymerizable deep eutectic solvents (PDESs).<sup>41–43</sup> In particular, PDESs are attracting significant attention due to their environmentally friendly nature and the tunable properties of the resultant ionic polymers that can eventually solve the leakage of liquid components that is a problem of ionogels and eutectogels. Most of these eutectic polymers feature good ionic conductivity, high elasticity, and potential biosafety as they are prepared from non-toxic precursors, perfectly matching the main bioelectronics demands.

In this review, we primarily analyze the most relevant advances in dry ionic conductive elastomers (ICEs) for bioelectronics synthesized from PDESs. First, we will introduce the concept of DESs and discuss the main points of this topic. Next, we will focus on the emerging types of PDES prepared from multifunctional building blocks, providing them with innovative properties, and will go into the main features of the resulting ionic polymers. Finally, we will highlight the emerging trends and future perspectives of this exciting realm.

## 2. Deep eutectic solvents (DESs): a thermodynamic point of view

The discovery of eutectic systems dates back to the 19th century when F. Guthrie described the “Eutexia” phenomenon in mixtures of two or more components showing a minimum liquefaction temperature at a particular composition (eutectic point).<sup>44</sup> Nowadays, it is known that all mixtures of pure compounds that are entirely or partly immiscible in the solid phase and miscible in the liquid phase present a eutectic point.<sup>45</sup> However, in 2003, Abbot *et al.* reported an abnormally large melting point depression in the mixture dubbed “reline” (melting point,  $T_m \approx 12^\circ\text{C}$ ), a combination of choline chloride (ChCl,  $T_m \approx 302^\circ\text{C}$ ) and urea (U,  $T_m \approx 133^\circ\text{C}$ ) at a 1:2 mol fraction.<sup>46</sup> This landmark study coined the term DES and postulated the hydrogen bonding between the mixture components, typically called a hydrogen bond donor (HBD) and hydrogen bond acceptor (HBA), as the root cause of their unexpected liquid behavior.

To date, there has been no firm consensus on the differences between traditional eutectic solvents and DES, and an established working definition for these neoteric systems is missing in the scientific community. Substantial progress has been made by Couthino *et al.*, who defined DES from the thermodynamic point of view as eutectic solvents whose components present enthalpic-driven negative deviations from ideality (see Fig. 1),<sup>47</sup> as this behavior is observed in the archetypical reline, which shows asymmetrical deviations in the urea liquidus curve. In general terms and for a binary mixture of components A and B, negative deviations occur when the interactions between them are stronger than the interactions with themselves in the pure state ( $A-B > A-A, B-B$ ). Therefore, marked negative deviations from thermodynamic ideality could create low-temperature melting mixtures, providing unusual liquid environments for new chemistries.

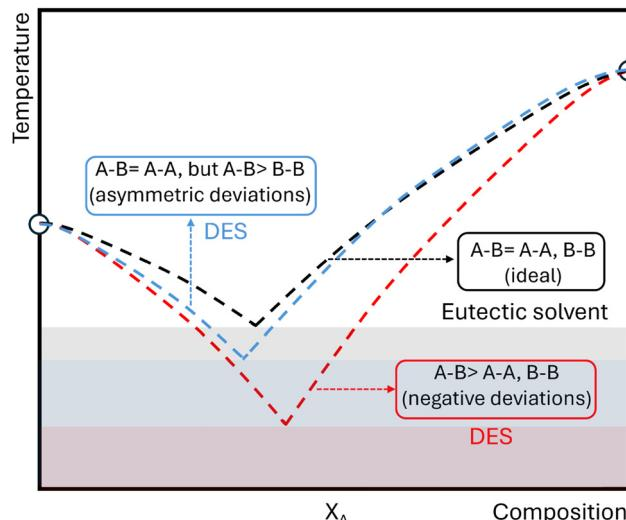


Fig. 1 Schematic illustration of solid–liquid equilibrium phase diagrams for mixtures of components A and B showing thermodynamic ideal behavior (dashed black line) or negative (dashed red line) or asymmetric (dashed blue line) deviations from thermodynamic ideality. Melting point depressions due to ideal liquid-phase behavior is an example of a eutectic solvent, while depression due to a negative non-ideality in the liquid phase is the case of a deep eutectic solvent. Adapted from ref. 47.

Despite these efforts, an important question remains: how significant should the magnitude of the negative deviations be for the eutectic mixture to be regarded as a DES? Many recent studies overlooked this point, and others labeled eutectic mixtures as DES even without knowing their solid–liquid equilibrium phase behavior. In this matter, van den Bruinhorst and Costa Gomes have recently proposed an empirical descriptor ( $D_e$ ) that can assist the classification of DESs, quantifying the eutectic depth.<sup>48</sup> This is an important first step, although a strict definition of DES based on  $D_e$  still requires setting an arbitrary threshold value. In our opinion, we should go back to the origins and call all the mixtures (deep or not) just eutectic solvents, as the relevant point is that they can be in a liquid state at a desired working temperature beyond their thermodynamic behavior. This ultimately enables tailored solvation environments and novel chemical reactions when they serve as solvents.

Another controversial point in the literature is whether mixtures that show a glass transition temperature ( $T_g$ ) in a broad composition range instead of a melting point can be defined as a DES, as is the case of several systems labeled PDES, as we will discuss later. Some authors have used the term low-transition-temperature mixtures (LTTMs) to define them,<sup>49</sup> and they may be treated outside of the DES family, although we will not make this distinction in this review.

### 3. Polymerizable deep eutectic solvents (PDESs): types and properties

PDESs are DESs that contain a polymerizable functional group, typically a (meth)acrylic moiety, and can be used as monomers.

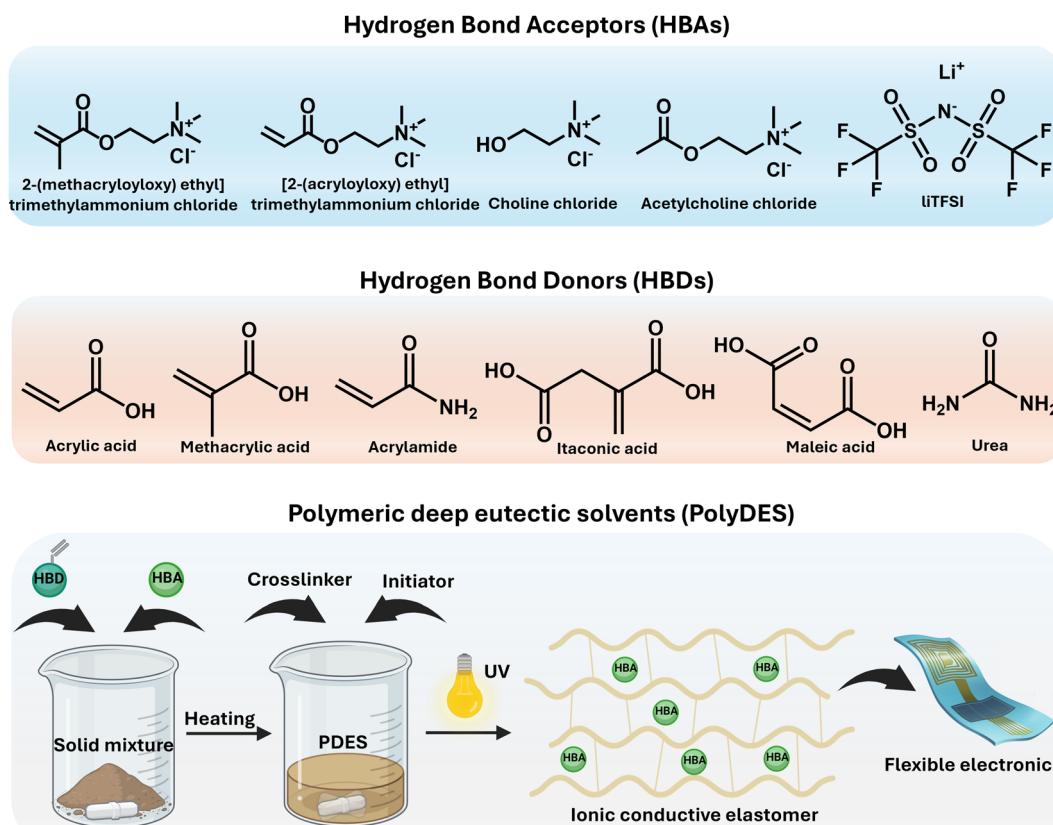
Liquid PDES monomers usually undergo a free-radical polymerization process while taking part in a DES, being applied to design new ionic polymers named polyDESs.<sup>50,51</sup> In these systems, the eutectic solvent plays a dual role as the reaction media and the reactant. At this point, it is noteworthy to mention that the reactive component of a PDES is consumed upon polymerization, leaving behind the inert component embedded in the polymer product and losing its liquid state. This is not a minor issue to be considered, as some recent work has wrongly labeled polyDES as a “gel” and *vice versa*, as we will discuss later, making it more challenging to undertake a profound revision of the field. Traditional PDESs rely on mixtures of neutral HBD monomers such as itaconic acid (IA), maleic acid (MA), acrylic acid (AA), methacrylic acid (MAA), hydroxyethyl methacrylate (HEMA), and acrylamide (AAm), among others, with HBA ammonium salts.<sup>52–55</sup> After polymerization, the resulting ionic polymers exhibit a homogeneous composition despite the absence of any solvent during the process. Mota-Morales *et al.* pioneered this PDES class, reporting the thermal frontal polymerization of AA/ChCl and similar PDESs.<sup>56,57</sup> More recent advances by Li *et al.* have unveiled the impact of hydrogen bonding interaction energy on the polymerization kinetics of these systems, exploring an array of quaternary ammonium salt homologs and AA.<sup>58</sup>

On the other hand, the second class of PDES consists of polymerizable ammonium salts and appropriate HBDs, like organic acids and amine compounds. Isik *et al.* first introduced the free-radical polymerization of PDES based on cholinium bromide methacrylate and renewable chemicals such as citric acid, malonic acid, and maleic acid, among others.<sup>59</sup> These eutectic monomers were liquid at room temperature and, like many others, showed an apparent  $T_g$  and no melting point. More recently, Mori *et al.* reported the preparation of a PDES by combining urea with commercial quaternary ammonium monomers, including methacryloylcholine chloride, diallyldimethyl ammonium chloride, and 2-(acryloyloxy)ethyl trimethyl ammonium chloride.<sup>60</sup>

These PDES examples benefit from tuneable viscosity and relatively low vapor pressure, allowing polymerizations at unavailable conditions for traditional organic solvents or water, besides offering a greener alternative for being all-in-one systems (solventless or bulk conditions). Scheme 2 summarizes the chemical structures of typical HBDs and HBAs used for PDES preparation and illustrates the synthesis of polyDES by photopolymerization, resulting in ICEs for flexible electronics.

Regrettably, most PDESs show limited functional features beyond their intrinsic ionic conductivity, and recent scientific efforts have been devoted to seeking innovative active components for multifunctional material design. General routes to improve the PDES properties include the addition of monomers for chemical cross-linking or H-bonding forming molecules for physical cross-linking.

For instance, de Lacalle *et al.* recently proposed polyphenols as building blocks of PDES (Fig. 2(A)).<sup>61</sup> These emerging materials can be tuned from adhesive to elastomers thanks to the chemical versatility of the natural phenolic molecules.



**Scheme 2** Examples of chemical structures of hydrogen bond acceptors (HBAs) and donors (HBDs), which have been combined to obtain PDESs (top). Schematic illustration of polyDES preparation by UV-photopolymerization resulting in ionic elastomers for flexible electronics.

Besides, the resulting polymers display bioactive properties stemming from the polyphenols, such as antimicrobial activity, and have an extraordinary ability for metal-ligand coordination. In the same line, Zhou *et al.* prepared antibacterial polyDES from a ternary PDES based on natural tannic acid (TA), ChCl, and HEMA.<sup>62</sup> In another exciting study, Thickett *et al.* proposed thermoresponsive polymer gels from PDES based on *N*-isopropylacrylamide and ChCl or acetylcholine chloride (AcChCl).<sup>63</sup> These materials featured a reduced swelling capacity and increased mechanical strength compared to those prepared by aqueous polymerization because of the significant increase in cross-linking density. Hoa *et al.* have recently reported the first luminescent polyDES prepared from a PDES based on AAm and SbCl<sub>3</sub>, which was utilized as a fluorescent anti-counterfeit ink, successfully used in fluorescence encryption (Fig. 2(B)).<sup>64</sup>

Altogether, the possibility of tailor-made composition of PDES from the vast library of HBD and HBA allows the fabrication of polyDES with a broad range of properties, from adhesives to dry elastomers. These traits and their intrinsic ionic nature have driven a new era of soft ionic materials that have found multiple applications in the bioelectronic field. The following section presents and discusses a detailed description of these systems as wearable electronic devices published over the last few years.

## 4. Dry ionic elastomer polyDESs in bioelectronics

### 4.1 polyDES elastomers from traditional PDESs

Soft ionic materials immobilizing an ionically conducting liquid phase, including hydrogels, ionogels, and eutectogels, suffer from critical limitations, such as freezing at extreme temperatures and leakage when subjected to mechanical stress.<sup>65</sup> Although the emergence of ionogels and eutectogels has alleviated some drawbacks, several challenges require new materials designs. The arrival of dry ionic conductive elastomers (ICEs) based on polyDES has changed the panorama of ionotropic devices, achieving precision and reliability for recording conductivity/resistance changes under harsh conditions.<sup>43</sup> The ion-solvation capacity of the polymer network allows the dry ICEs to exhibit good ionic conductivity while preserving their elasticity and flexibility. This point is favorable in PDES, where ion miscibility is highly probable due to the compatibility of the HBD and HBA in the liquid phase. This represents a considerable advantage compared to standard methods for obtaining ICEs, which involve blending solid salts into the polymer matrix,<sup>66</sup> and can lead to macroscopic phase separation. For this reason, PDES are increasingly being used to design liquid-free ICEs. The Minghui He's group significantly advanced in this field, exploring different ICEs based on

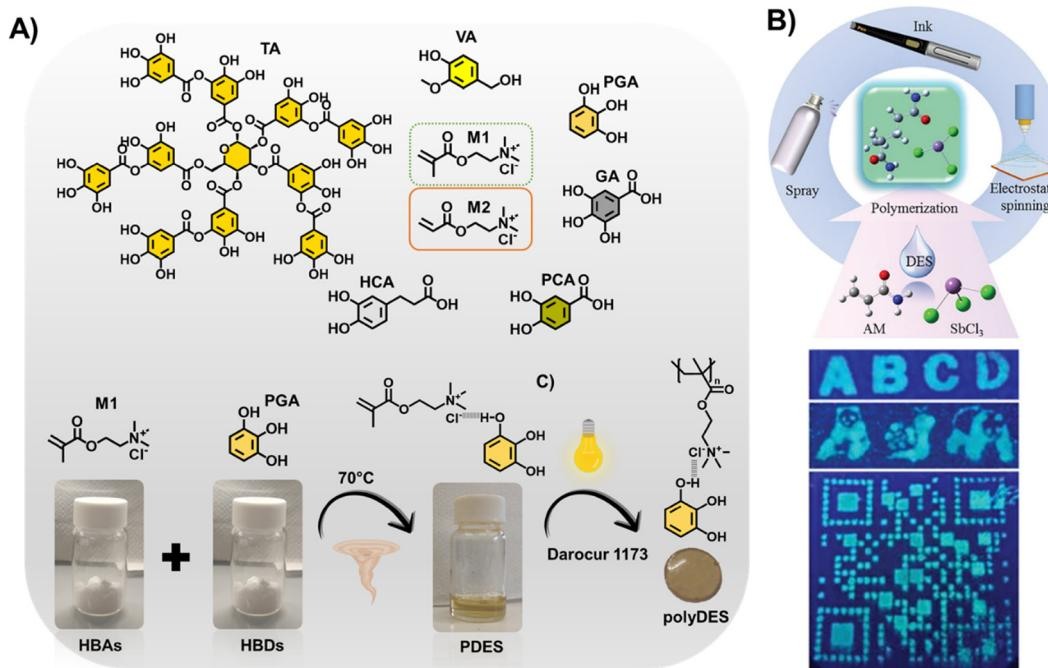


**Fig. 2** (A) Structure of polyphenols and quaternary ammonium monomers used for multifunctional PDES (top) and schematic representation of the PDES preparation procedure and photopolymerization step to fabricate phenolic polyDES (bottom). TA: tannic acid, VA: vanillyl alcohol, PGA: pyrogallol, GA: gallic acid, HCA: hydrocaffeic acid, PCA: protocatechuic acid, M1: [2-(methacryloyloxy) ethyl] trimethylammonium chloride, M2: [2-(acryloyloxy) ethyl] trimethylammonium chloride. Adapted from ref. 61 with permission from the American Chemical Society. (B) Schematic illustration of polymerization-induced fluorescence in polyDES and its anti-counterfeiting application (top). Images of filter papers impregnated with poly(AAm/SbCl<sub>3</sub>) showing fluorescent patterns under UV light (bottom). Adapted from ref. 64 with permission from Wiley-VCH GmbH.

neutral monomers/quaternary ammonium salt PDESSs. For instance, they developed 3D patternable and transparent elastomers based on the mixture of AA : ChCl (2 : 1 mole ratio,  $T_m = -5$  °C).<sup>67,68</sup> These polyDESSs were obtained by photopolymerization using polyethylene glycol diacrylate (PEGDA) as the crosslinker (1–5 wt%) and Irgacure 2959 as the UV photoinitiator, showing acceptable stretchability (strain up to 150%) and good conductivity ( $\approx 0.2$  S m<sup>-1</sup>). The polyDES was 3D-shaped in a starfish architecture (Fig. 3(A) and (B)) and integrated into a tactile sensor, displaying good sensitivity to detect pressure values ranging from 220–1400 Pa (Fig. 3(C)). Moreover, these elastomers could also be used in strain sensors to monitor human motions, as shown in Fig. 3(D), where the electrical resistance variation is followed over time when the polyDES is attached to an index finger and bent at different angles (Fig. 3(D)). In follow-up articles, these authors designed electroconductive hybrid materials filling the channels and pores of delignified wood or a nanopaper substrate made of cellulose nanofibrils with this polyDES *via* *in situ* photopolymerization, which provided the materials with stretchability ( $\approx 7$ –80% strain) and good ionic conductivity (0.13–0.16 S m<sup>-1</sup>).<sup>69,70</sup> These hybrid ionic composites exhibited impressive functional sensing abilities to external stimuli, including pressure and strain.

#### 4.2 Dynamic polyDES elastomers from multifunctional crosslinkers

Recent research efforts have focused on improving the mechanical properties of dry elastomers and providing them with

self-healing properties. Apart from the chemical crosslinkers bearing (meth)acrylate functionalities, one attractive strategy explored includes multifunctional molecules with a hydrogen bonding ability in the PDES formulation to synergize dynamic interactions and covalent bonds. For example, Li *et al.* used phytic acid in the archetypical AA : ChCl (2 : 1 mole ratio) PDES combined with PEGDA to fabricate transparent ultrastretchable ( $\approx 1300\%$  strain) polyDES ( $T_g$  ranging from  $-53.5$  °C to  $-74.3$  °C) with good strength ( $\approx 0.45$  MPa) and a fast self-healing ability (within 2 s).<sup>71</sup> The authors found that only polyDES/phytic acid showed effective self-healing compared to polyDES alone and a poly(AA)/phytic acid mixture. With an excellent self-healing efficiency (91.5% within 48 h), these dynamic elastomers could follow the bending of a finger joint and detect small vibrations caused by human vocalization (figure, showing almost identical signal patterns before damage and after healing for 24 h).

In a follow-up article, the authors replaced ChCl in this formulation with tetramethylammonium chloride (TMAC) (PDES  $T_m$  = ranging from  $-12.7$  °C to  $-20.3$  °C), reaching the highest mechanical performance reported for ICEs to date, with a tensile strength, strain at break, and toughness of 31.21 MPa, 3645%, and 615 MJ m<sup>-3</sup>, respectively (Fig. 4(A)).<sup>72</sup> Phytic acid allows easy modulation of the stretchability of these elastomers, which varied from 22% to 6164% with concentrations of this natural molecule from 0 to 15 wt%. Ionic conductivity also changed from 0.007 to 0.037 S m<sup>-1</sup> for this concentration range. The authors demonstrated by density functional theory

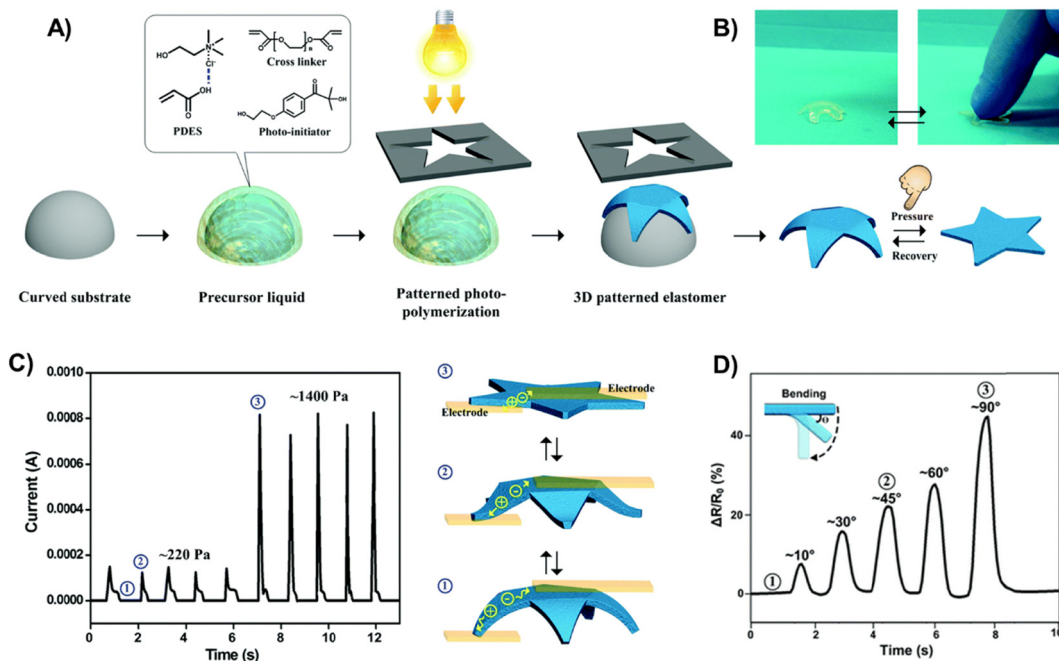


Fig. 3 (A) Schematic illustration of fabricating a starfish-shaped 3D polyDES architecture. (B) Digital images of this 3D architecture reversibly deforming without (left)/with (right) external pressure. Plot of the resistance of 3D polyDES architectures as a function of time when subjected to pressure (C) and bending deformation (D). Adapted from ref. 67 with permission from the Royal Society of Chemistry.

(DFT) modeling that the extraordinary mechanical behavior of these elastomers is because of intermolecular solid interactions (dynamic bonds) between TMAC and phytic acid. When this dynamic elastomer was cut into two pieces (Fig. 4(B), left), it recovered electrical conductivity immediately after they were brought into contact, recovering to 99% of its initial value within 0.26 s (Fig. 4(B), middle and right), demonstrating the impressive electrical self-healing ability provided by the multi-functional phytic acid. Indeed, microscopically analyzing the damaged elastomers revealed that hydrogen bonds allow polymeric chains to inter-diffuse across fractured interfaces and cross-links reformation, gradually disappearing the cutting scar after 24 h (Fig. 4(C)). The polyDESs were then integrated into running shoes to monitor different human motions (stand, walk, and jump) with great sensitivity. Furthermore, the sensor showed excellent stability, maintaining constant electrical signals for over 7000 cycles under 50% strain.

Similarly, self-healing and transparent flexible electronics from a ternary eutectic mixture of AA, ChCl, and  $\text{AlCl}_3 \cdot 6\text{H}_2\text{O}$  ( $T_g = -100^\circ\text{C}$ ) were also developed.<sup>73</sup> In these materials, the hydrated metal halide was introduced for ion coordination with carboxylic groups of the monomers, reaching dynamic interactions that allowed high stress at break ( $\approx 5$  MPa), excellent stretchability ( $\approx 900\%$ ), and good self-healing efficiency ( $\sim 82.8\%$  in 72 h at room temperature without an external stimulus). Furthermore, unlike other metal cations, such as  $\text{Fe}(\text{m})$ ,  $\text{Al}(\text{m})$  gives transparent and colorless polyDESs. These elastomers were further covalently cross-linked with PEGDA, where this dual cross-linking strategy produced mechanically tough networks ( $\approx 22$  MJ m $^{-3}$ ). With ionic conductivity values

of  $9 \times 10^{-3}$  S m $^{-1}$ , these polyDES performed well as strain sensors to monitor human motions.

#### 4.3 Copolymeric polyDES elastomers from ternary PDES mixtures

Another smart approach to modulate the elastomeric and self-healing behavior of polyDES is the copolymerization of soft and hard monomers using ternary PDES mixtures. Minghui He's group pioneered this concept by fabricating elastomers based on AAm:MA:ChCl PDES ( $T_g = -72.5^\circ\text{C}$ ) (Fig. 5(A)).<sup>74</sup> In these materials, the hard poly(AAm/ChCl) chain segments increased the mechanical strength and  $T_g$  (ranging from  $-72.2$  to  $-92.8^\circ\text{C}$ ), while the soft poly(MA/ChCl) promoted the flexibility of the polymeric network. The resulting elastomers showed good elasticity (strain up to 450%) and strength (stress at break up to 0.65 MPa), good conductivity ( $4.0 \times 10^{-2}$  S m $^{-1}$ ), and self-healing (healing efficiency up to 94% in 72 h at  $60^\circ\text{C}$ ) over a wide temperature range ( $-23$  to  $60^\circ\text{C}$ ) thanks to the formation of strong hydrogen bonding interactions. It was demonstrated that these polyDESs could be used as movement sensors with reliable recording over a wide temperature range ( $-23$ – $60^\circ\text{C}$ ) even after being damaged and healed (Fig. 5(B)). Then, the authors extended this concept to AA:MA:ChCl ternary PDES mixtures ( $T_g = -78.3^\circ\text{C}$ ), obtaining poly(AA/ChCl-*co*-MA/ChCl) copolymers ( $T_g$  ranging from  $-57.4$  to  $-75.1^\circ\text{C}$ ) that outperformed the poly(AAm/ChCl-*co*-MA/ChCl) elastomers in terms of stretchability (strain up to 1450%), and excellent ionic conductivity ( $0.43$  S m $^{-1}$ ), but with limited strength (stress at break up to 0.18 MPa).<sup>75</sup> This fact suggests that in these types of dynamic copolymers,  $-\text{COOH}/-\text{COOH}$  interactions are weaker

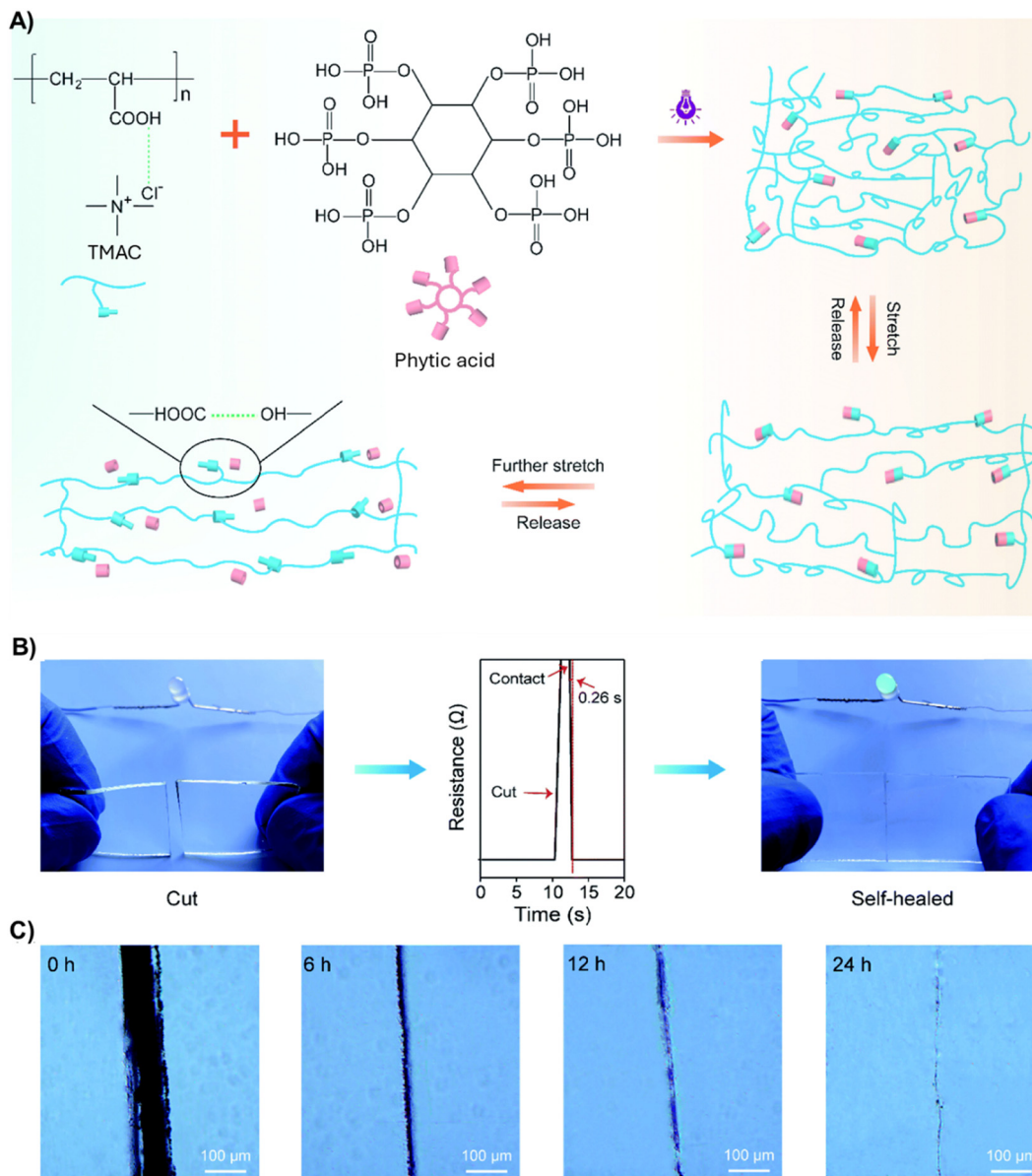
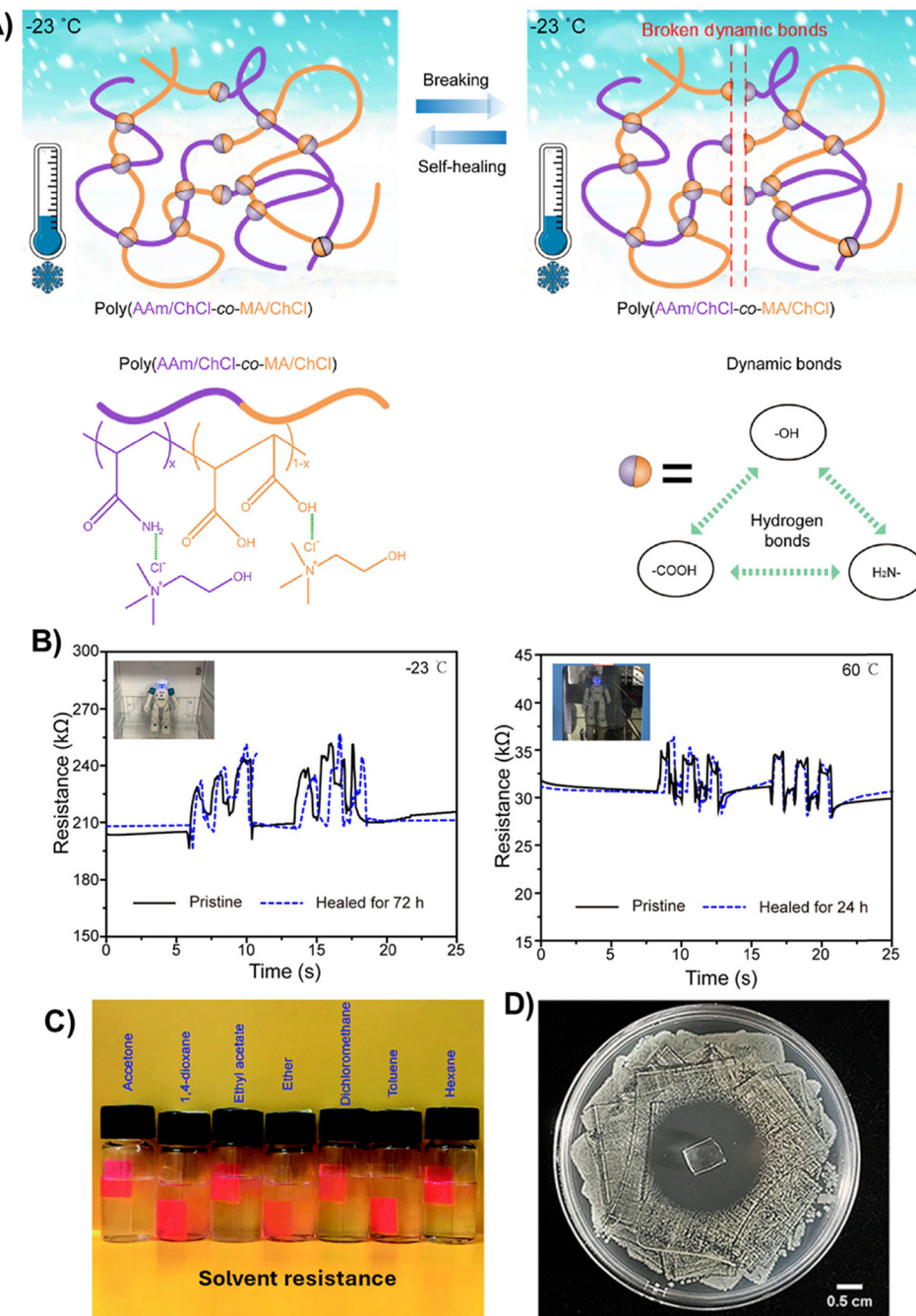


Fig. 4 (A) Schematic illustration of the extremely tough and ultra-stretchable polyDES based on TMAC, AA, and phytic acid molecules. (B) Digital images of the electrical self-healing process for a broken ICE in series with an LED. The film's resistance could recover rapidly to its original value without external stimuli within 0.26 s. (C) Optical microscope images of the self-healed ICE (10 wt% phytic acid) at room temperature for 24 h. Adapted from ref. 72 with permission from the Royal Society of Chemistry.

than  $-\text{COOH}/-\text{NH}_2$  ones, even though the authors found almost identical solvation electronic energy for both systems;  $-18.0 \text{ kcal mol}^{-1}$  for poly(AA/ChCl-*co*-MA/ChCl) vs.  $-18.3 \text{ kcal mol}^{-1}$  for poly(AAm/ChCl-*co*-MA/ChCl). Interestingly, dynamic interactions in poly(AA/ChCl-*co*-MA/ChCl) elastomers provided them with organic solvent resistance (Fig. 5(C)), maintaining their morphology and self-healing properties in acetone to hexane for 24 h. These polyDESs also showed excellent recording sensitivity when integrated into movement soft sensors after healing even in acetone for 24 h, opening new pathways for autonomous self-healing IECs. Similarly, Sang *et al.* introduced acrylamide-2-methylpropanesulfonic acid (AMPS) as a hard monomer in

the archetypical AA/ChCl PDES system, modulating the  $T_g$  of the polyDES from  $-72.7 \text{ }^\circ\text{C}$  to  $-93.7 \text{ }^\circ\text{C}$ .<sup>76</sup> Because the AMPS monomer contains the sulfonic acid group ( $-\text{SO}_3\text{H}$ ) with strong hydrogen bond interaction ability, these elastomers showed excellent mechanical strength (5.7 MPa) and stretchability (870%), fast self-healing (within 4 h for complete mechanical recovery) and ionic conductivity of  $0.7 \times 10^{-2} \text{ S m}^{-1}$ .

Inspired by these studies, more recently, Jin *et al.* prepared poly(AA/ChCl-*co*-IA/ChCl) elastomers ( $T_g$  ranging from  $-16$  to  $8 \text{ }^\circ\text{C}$ ) (Fig. 5(A)).<sup>78</sup> Using even a small amount of IA in the PDES formulation (AA:IA:ChCl = 2:0.3:1 mole ratio) produced polyDES with superb mechanical properties (maximum strain and stress at break of around 1456% and 5.3 MPa, respectively),



**Fig. 5** (A) Demonstration of the healing process and chemical structure of poly(AAm/ChCl-co-MA/ChCl) elastomers (bottom left). Hydrogen bonds between binary building blocks of the poly(AAm/ChCl-co-MA/ChCl) system (bottom right). (B) Time evolution of the electrical signal when the elastomers were integrated upon the knee of a robot to record its movements at -23 °C in a refrigerator (left) and 60 °C in an oven (right). Adapted from ref. 74 with permission from the American Chemical Society. (C) The poly(AA/ChCl-co-MA/ChCl) elastomers healed in various organic solvents. Adapted from ref. 75 with permission from the Royal Society of Chemistry. (D) Antibacterial properties of poly(AA/ChCl/IA/DMA) determined by the bacteriostatic circle method against *E. coli*. Adapted from ref. 77 with permission from the Royal Society of Chemistry.

revealing the superior ability of this dicarboxylic acid for hydrogen bonding compared to MA and AMPS. However, higher non-covalent cross-linking in these elastomers could stunt the free movement of ions, negatively affecting their ionic conductivity, which was  $2.76 \times 10^{-4}$  S m<sup>-1</sup>, significantly lower than those for poly(AAm/ChCl-co-MA/ChCl) and

poly(AA/ChCl-co-MA/ChCl). The authors fabricated strain sensors with these elastomers, showing high sensitivity, small hysteresis, and good cyclic stability to monitor human motions. A later study by Wu *et al.* introduced *N,N*-dimethylacrylamide (DMA) into the AA/IA/ChCl PDES system, seeking to strengthen the polyDES network.<sup>77</sup> These improved elastomers reached an

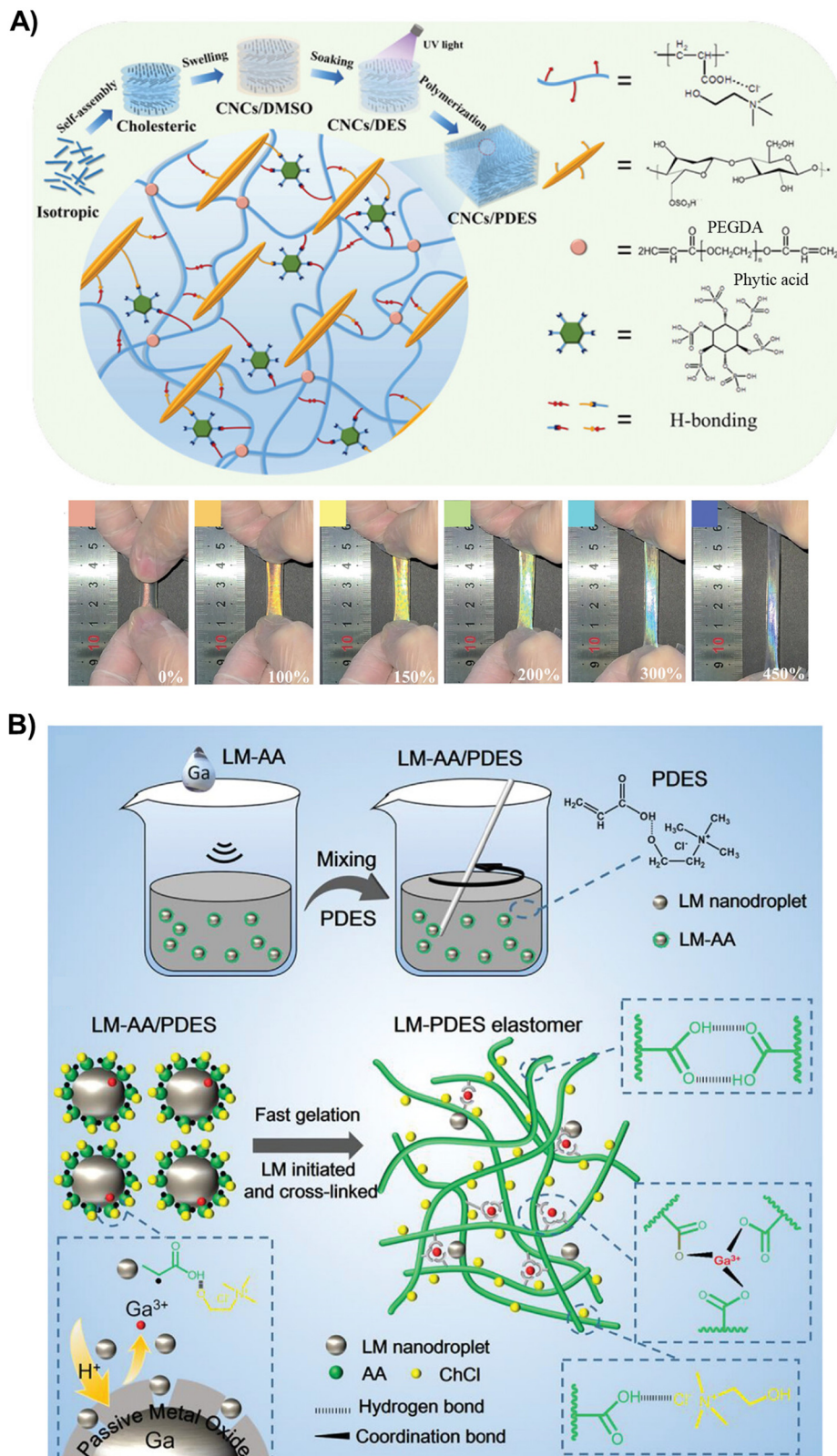


**Fig. 6** (A) Schematic illustration for preparing CNC/polyDES *in situ* composites and network of dynamic interfacial hydrogen bonds (top). Digital photos of the CNC/polyDES elastomer ( $20 \text{ mm} \times 8 \text{ mm} \times 1.7 \text{ mm}$ ) during the stretching process (scale bars:  $100 \mu\text{m}$ ) (bottom). Adapted from ref. 83 with permission from Wiley-VCH GmbH. (B) Schematic diagram of the preparation method of LM-polyDES elastomers cross-linked by  $\text{Ga}^{3+}$  ions. Adapted from ref. 84 with permission from Wiley-VCH GmbH.

outstanding tensile strength of  $\approx 21$  MPa and a stretchability of  $\approx 559\%$ . The ionic conductivity was also enhanced by two orders of magnitude up to  $0.04$  S m $^{-1}$ . The ICE was used to manufacture a wearable sensor that can detect pressure changes and human movement in the finger, knee, throat, and other parts. More interestingly, the authors studied the antibacterial properties of these elastomers against *E. coli*, revealing a potent bactericidal performance, which was attributed to ChCl and IA (Fig. 5(D)). This is essential for long-term recording, considering the possibility of bacteria colonization on the skin.

Beyond the above-discussed systems, only a few other ternary PDES, including functional monomers, have been proposed so far. For instance, Chen *et al.* reported ChCl:AA:1-vinyl imidazole mixtures (1:2:0.15 mole ratio,  $T_g = -39$  °C), obtaining polyDES with a stretchability, toughness, and conductivity of  $\approx 1500\%$ ,  $3.15$  MJ m $^{-3}$ , and  $3.2 \times 10^{-4}$  S m $^{-1}$ , respectively.<sup>79</sup> More recently, Liu *et al.* prepared polyDESs based on ChCl:AA:hydroxyethyl acrylate (HEA), obtaining dry elastomers with good stretchability (511%) and toughness (71 MJ m $^{-3}$ ), although these materials were labeled as eutectogels.<sup>80</sup> The authors attributed this good mechanical performance to microphase separation in the ionic polymer.

#### 4.4 Nanocomposite polyDES elastomers

Besides controlling the chemical composition of the polyDES, recent research has focused on enriching the ICEs with different nanofillers to form nanocomposites. In various forms, such as nano and microfibers and nanocrystals, cellulose is perhaps the most used reinforcer in polyDES formulations. In one pioneering work, Qi *et al.* incorporated bacterial cellulose nanofibers (BC) in the archetypical AA:ChCl PDES, resulting in a polyDES with improved mechanical performance (290% of strain, 0.8 MPa of stress, and  $1.86$  MJ m $^{-2}$  of fracture energy) but still far from other ICEs previously discussed.<sup>81</sup> The calculated conductivity for these elastomer nanocomposites was around  $0.18$  S m $^{-1}$ , and they could effectively work as strain and movement sensors. Similarly, Jiang *et al.* strengthened AA:ChCl polyDES with cellulose microfibers obtained by hydrolysis of kraft pulp in this PDES. The authors demonstrated that only 1 wt% of filler is enough to reach a tensile strength, strain at break, and toughness of 0.46 MPa, 3210%, and  $13.17$  MJ m $^{-3}$ , respectively.<sup>82</sup> These good mechanical parameters were attributed to a reorientation and alignment of the microfibers in parallel along the stretching direction. During deformation, the mechanical load was transferred along the oriented nanofiller due to good interfacial bonding with the polyDES network, dissipating energy.

In another exciting work, Tian *et al.*, inspired by the skins of a chameleon, designed schemochrome elastomers by embedding a cellulose nanocrystal (CNC, 360 nm length) cholesteric skeleton into AA:ChCl polyDES (Fig. 6(A), top).<sup>83</sup> Furthermore, phytic acid was used as a small molecule hydrogen bond regulator to establish a flexible and untangled polymeric network. In this interesting blueprint, CNC were self-assembled into an iridescent cholesteric liquid crystal film and soaked in

the PDES, previous DMSO swelling, and solvent replacement. The orientation of the CNC could change from chiral nematic order in a relaxed film to a partially aligned arrangement when stretched, modifying the helical pitch cholesteric skeleton and, consequently, the wavelength of the reflected light, which provides a strain-responsive color-changing ability to the polyDES (Fig. 6(A), bottom). The nanocomposites' maximum strain, tensile strength, and fracture toughness are 1163.7%, 0.59 MPa, and  $3.66$  MJ m $^{-2}$ , respectively. These flexible ionic conductive elastomers can work as resistive sensors to capture human real-time motions.

In the same direction, Yang *et al.* fabricated ICEs incorporating tannic acid (TA)-decorated CNC (TA@CNC) in AA:ChCl polyDES cross-linked with *N,N'*-methylenebisacrylamide.<sup>85</sup> In these elastomers, TA@CNC plays a dual role; the cellulose rigid core acts as a reinforcer, while TA can form multiple hydrogen bonds with the polyDES, providing a dynamic network for energy dissipation. These ICEs featured good stretchability (up to 2400%), mechanical strength ( $\approx 0.5$  MPa), toughness (3.44 MJ m $^{-3}$ ), adhesion strength (68 kPa), self-healing (healing efficiency of 53% in 72 h at 30 °C), anti-freezing properties (operation over a wide temperature range, -40 to 60 °C), and high ionic conductivity (0.38 S m $^{-1}$ ). Moreover, the polyDESs were used for designing pressure and strain sensors showing a broad detection range ( $\approx 1$ –300 kPa), good sensitivity (12.55 MPa $^{-1}$ ), and reliable electromechanical response over 1000 cycles of strain-relaxation. Following a similar strategy, Jiang *et al.* recently proposed the derivatization of CNC (164 nm length and 10.0 nm width) by introducing more primary hydroxyl groups (DCNC) to improve their dispersibility in the AA:ChCl PDES and consequently increase the nanofiller concentration in the polyDES.<sup>86</sup> The fully physically cross-linked nanocomposite elastomer with 2 wt% of DCNC showed fracture strain up to 3869% and a tensile strength of 0.22 MPa. Furthermore, these ICEs exhibited an excellent sensing ability with a wide sensing range (up to 2000% strain) and low detection limit (1% strain). The derivatization of cellulose with methacrylate groups to yield a macro-crosslinker of an AA:ChCl:urea mixture was also recently proposed,<sup>87</sup> but, although the authors defined these materials as liquid-free elastomers, the pair ChCl:urea is not a reactive DES which remains within the network after polymerization, resulting in a eutectogel rather than a dry ICE.

Besides cellulose, other types of nanoreinforcers have scarcely been explored in the literature for polyDES so far. In one exciting example, a liquid metal (LM) eutectic mixture of gallium (75 wt%) and indium (25 wt%) (EgaIn) was dispersed as 500 nm droplets within the AA:ChCl PDES.<sup>84</sup> When applying ultrasound, the LM can generate free radicals to initiate the polymerization, while Ga $^{3+}$  ions released from the metal droplets can coordinate with the COOH groups of AA for polyDES cross-linking (Fig. 6(B)). The resulting elastomers with an LM content below 1 wt% display ultrastretchability (2600%), high toughness (2.36 MJ m $^{-3}$ ), good ionic conductivity (0.13 S m $^{-1}$ ), and resistance to freezing and drying, enabling them to operate as strain sensors under harsh conditions up to -40 °C.

More recently, Zhang *et al.* hydrolyzed TA by ultrasonication into ellagic acid (EA), and then  $\text{Fe}^{3+}$  was introduced to induce the complexation of the phenolic molecules into aggregated nano-spheres (EAN, 60–140 nm in diameter) through metal-hydroxyl coordination.<sup>88</sup> The EAN were dispersed into a PDES based on AA and maleic anhydride (MAH) as soft and hard segments, respectively. The  $-\text{COOH}$  groups from polyDES can form dense hydrogen bond interactions with the catechols and gallol groups of the EAN, and coordinate with the residual  $\text{Fe}^{3+}$  on the surface of these nanoparticles, giving highly dynamic materials. Indeed, these polyDES nanocomposites ( $T_g = 35.75^\circ\text{C}$ ) reached an extraordinary self-healing ability at  $-20^\circ\text{C}$  (85.7% healing efficiency within 6 h), very high tensile strength ( $\approx 31\text{ MPa}$ ), good elasticity ( $\approx 300\%$ ), and superb toughness ( $\approx 70\text{ MJ m}^{-3}$ ). Although the polyDES featured relatively low conductivity, ranging from 0.1 to  $9 \times 10^{-3}\text{ S m}^{-1}$  in the temperature interval of  $-40$  to  $50^\circ\text{C}$ , they showed a good sensing ability even at  $-20^\circ\text{C}$ .

#### 4.5 Interpenetrated polymer networks based on polyDES

The interpenetrated double network (DN) strategy has been deeply explored for fabricating ultra-tough hydrogels where sacrificial bonds are designed to absorb the mechanical energy during fracture.<sup>89,90</sup> This attractive concept has recently been extended to polyDES, where linear polymers or cross-linked networks are interpenetrated within these elastomer materials for energy dissipation. He *et al.* first reported this approach in

AA:ChCl PDES incorporating polyvinylpyrrolidone (PVP) (2 wt%) as a hard physical network.<sup>91</sup> The resulting polyDES DN were highly transparent (transmittance = 92%) and showed outstanding mechanical performance, with tensile strength, strain at break, and toughness up to 71.3 MPa, 671%, and  $268\text{ MJ m}^{-3}$ , respectively. Furthermore, these ICEs have excellent self-healing properties with an electrical healing efficiency of 98% within 0.30 s. However, the PVP content negatively affected the ionic conductivity, ranging from  $3.1 \times 10^{-4}\text{ S m}^{-1}$  to  $1.8 \times 10^{-3}\text{ S m}^{-1}$  when the added polymer increased from 0 to 2 wt%. Nevertheless, the elastomers showed stable signal recording when evaluated as movement sensors. These authors later explored the interpenetration of polydopamine in the same PDES formulation. However, the resulting elastomers showed greatly diminished mechanical performance compared to PVP-based DN, with limited strength (0.58 MPa) and toughness ( $1.4\text{ MJ m}^{-3}$ ), although their elasticity (1200%) and ionic conductivity ( $2.31 \times 10^{-2}\text{ S m}^{-1}$ ) was improved.<sup>92</sup>

Similarly, He *et al.* also investigated the semi-interpenetration of lignin into a PDES formulation based on AA:cholinium dihydrogen citrate (CDC) (2:1 mole ratio) (Fig. 7).<sup>93</sup> In particular, CDC can form strong hydrogen bonds with poly(AA), while the introduction of lignin can further strengthen the polymer network. Besides providing a sacrificial structure for energy dissipation, lignin provided this elastomer with self-adhesive features. The materials' tensile strength, strain at break, and toughness were 13.59 MPa, 1013%, and

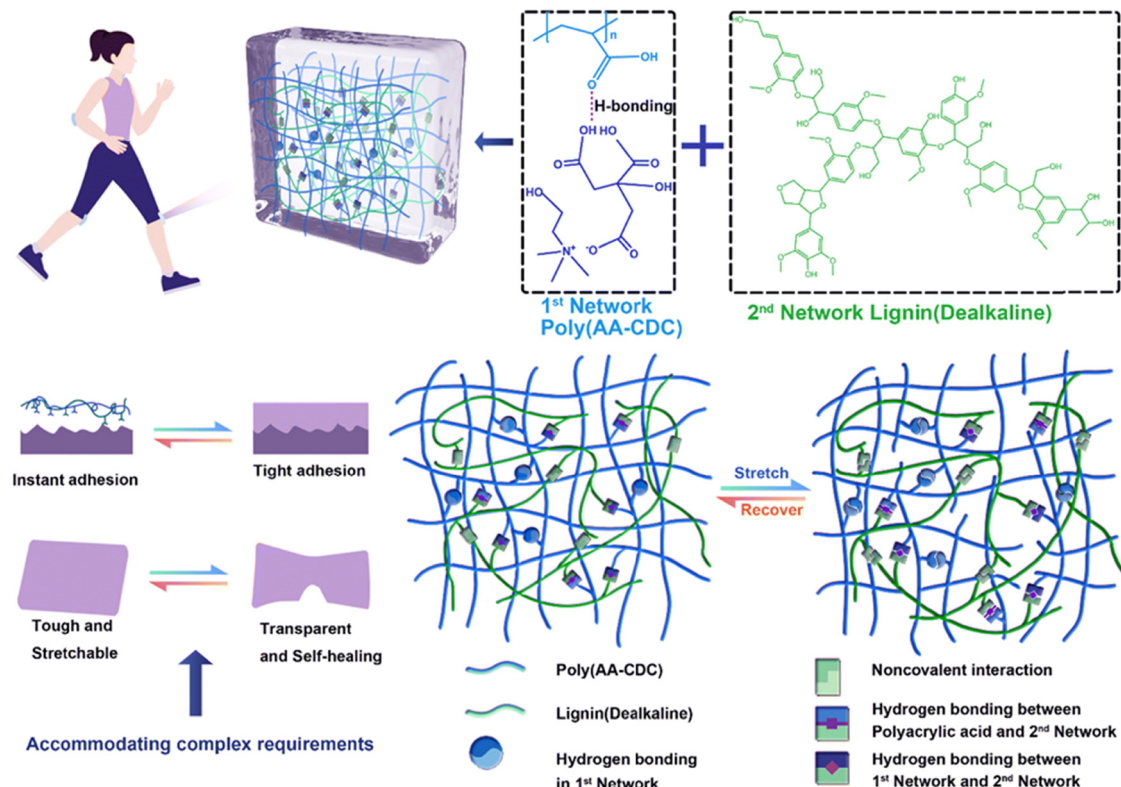


Fig. 7 Design concept and composition of poly(AA/CDC)/lignin elastomers (top), typical physicochemical properties (bottom left), and the interactions within the double-network (bottom right). Adapted from ref. 93 with permission from the Royal Society of Chemistry.

115.04 MJ m<sup>-3</sup>, respectively. In addition, they showed a strong electrical self-healing efficiency of up to 90% in 0.4 s at room temperature and good electrical conductivity (9.63 × 10<sup>-3</sup> S m<sup>-1</sup>).

In another work, Chu *et al.* fabricated double-network elastomers interpenetrating carboxymethyl chitosan (CMC) in a ternary PDES formulation based on AA, ChCl, and a vanillin-derived monomer (VAM) (2:1:0.1 mole ratio).<sup>94</sup> In these elastomers, the network inside the polyDES was created by Schiff-base chemistry between the aldehydes groups of VAM and the -NH<sub>2</sub> groups of CMC, rendering dynamic covalent bonds that provide self-healing properties (92.1% self-healing efficiency after healing 50 h). Despite the synthetic efforts, the mechanical parameters of these materials were modest, with tensile strength, strain at break, and toughness up to 1.48 MPa, 1475%, and 0.39 MJ m<sup>-3</sup>, respectively. Their ionic conductivity was also limited to 0.11 S m<sup>-1</sup>. The  $T_g$  of the polyDES was in the range of -40 °C to -60 °C, allowing good elasticity at below-zero temperatures (200% strain). These conductive elastomers were employed as a strain sensor and wearable device to monitor human motions, and their sensing capability was even maintained at -25 °C.

Hu *et al.* recently proposed an innovative strategy to construct an ultra-robust elastomer based on poly(vinyl alcohol) (PVA) semi-interpenetrated with AA:ChCl polyDES.<sup>95</sup> The synthetic blueprint for these materials relies on a preliminary step where PVA hydrogels are prepared using the traditional freezing-thawing method, followed by annealing at 40 °C first and then at 90 °C for water desolvation to induce PVA crystallization. After immersing in water for 24 h to extend polymer conformation and homogenize networks, the second step consisted of solvent exchange with the PDES and photopolymerization. These elastomers' tensile strength and maximum strain were 46.5 MPa and 250%, respectively. Although the

authors did not report the performance of the polyDES in wearable devices, they tested the eutectogel swollen with the PDES as an electronic ligament that can not only control and guide bone movements but also serve as a strain sensor.

#### 4.6 PolyDES elastomers from non-conventional PDES

Readers may have noticed that most of the polyDES elastomers in the literature are based on the archetypical AA:ChCl PDES, and only a few other neutral monomers or quaternary ammonium salts have been explored to date. Thus, there is an urgent need for innovative PDESs with new functionalities, and some recent works have tried to address this point. In the previous section, we already discussed the robust supramolecular polyDES developed from the AA:CDC PDES formulation, which was one initial promising step toward multifunctional hydrogen bond acceptors with a cross-linking capacity.<sup>96</sup> Subsequent studies have explored acetylcholine chloride as an alternative to the classical ChCl or TMAC, which can be combined with HEMA and a polyurethane macro-crosslinker to produce pressure sensitive ICES.<sup>97</sup> In other fascinating work, Liu *et al.* designed *N*-cyanomethyl acrylamide (NCMA) monomer able to form a PDES when mixed with bis(trifluoromethane) sulfonimide (LiTFSI) (Fig. 8(A)).<sup>98</sup> The polymerization step did not include chemical cross-linking agents, forming supramolecular polyDES by the hydrogen bonding interactions between amide groups and dipole-dipole interactions of the cyanide group in the side chain of the polymer (Fig. 8(B)). The resulting elastomers display a  $T_g$  between -48 °C and -54 °C, giving excellent mechanical properties with tensile strength, stretchability, and toughness around 13 MPa, 300%, and 30 MJ m<sup>-3</sup>, respectively. As a common denominator of many polyDES, the ionic conductivity of these elastomers was only 3.6 × 10<sup>-5</sup> S m<sup>-1</sup> at 30 °C and increased to 2 × 10<sup>-3</sup> S m<sup>-1</sup> at 90 °C. Interestingly, the authors used these polyDES to fabricate a wireless temperature

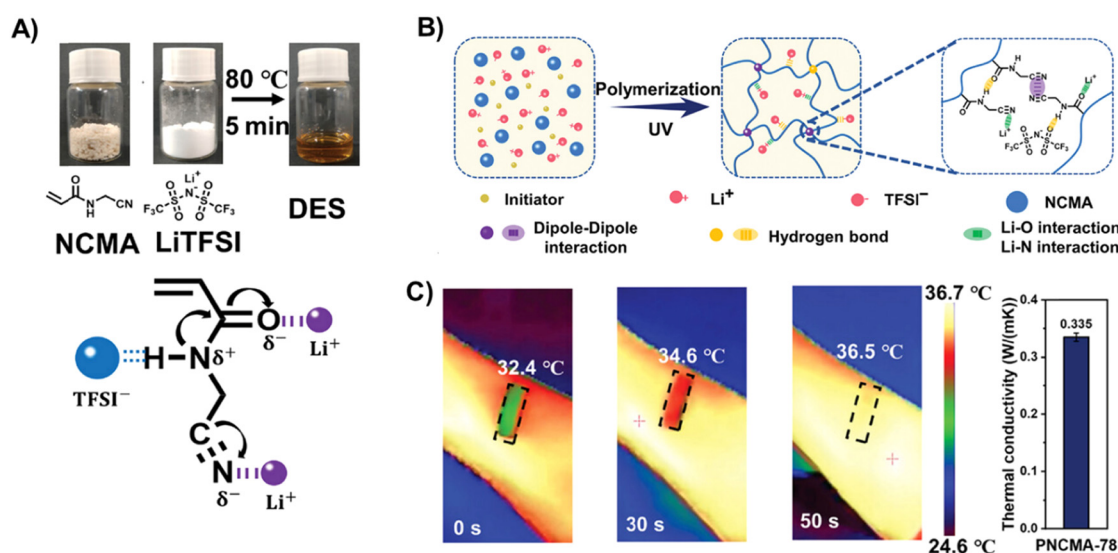


Fig. 8 (A) Preparation method for PDES using NCMA and LiTFSI and schematic representation of its interactions. (B) Schematic preparation diagram of the poly(NCMA/LiTFSI) elastomer. (C) Thermal infrared images (left) and thermal conductivity (right) of the poly(NCMA/LiTFSI) elastomer from a wireless body temperature monitor. Adapted from ref. 98 with permission from Wiley-VCH GmbH.

monitoring device (Fig. 8(C)), showing the highest value of temperature coefficient of resistance reported to date and unveiling the outstanding temperature sensitivity of these materials.

Other innovative recently proposed PDES formulations rely on the mixture of neutral monomers and ionic liquid salts, although technically, the resulting elastomers deserve the label of ionogels and will not be discussed in detail here. For instance, Ji *et al.* prepared PDES by mixing AA ( $T_g$  ranging from  $-40$  to  $-22$  °C)<sup>99</sup> or AAm ( $T_g = -64$  °C)<sup>100</sup> with 1-butyl-3-methylimidazolium chloride, an ionic liquid with a melting point of 70 °C.

#### 4.7 Additive manufacturing for PolyDES 3D structuring

The strong molecular interactions between the mixture components in PDES usually feature high viscosity, and potentially tunable rheological properties, opening opportunities to exploit them as reactive inks in different additive manufacturing techniques. Among them, 3D printing stands out as one of the most versatile ways to fabricate complex structures, while electrospinning can be used to produce conductive fibers. This section summarizes the recent progress made in this matter, highlighting the huge potential of PDES to design complex geometries using advanced manufacturing techniques of interest for the easy fabrication of bioelectronic components.

Prof. He's group has made great progress in this topic since 2021, investigating the structuring of polyDES by additive manufacturing. For instance, one of their copolymers based on AAm:ChCl:MA in different mole ratios (2:1:1, 2:1:2, 1:1:1, and 1:2:2) were 3D printed in transparent conducting elastomeric pressure sensors with a precision of 10 µm, having stable electrical signals at 50% compression for 10 000 cycles.<sup>101</sup> The authors demonstrated that the printed sensors could highly reproduce diverse designs, even of complex hollow frames, sharp peak structures, porous structures, and hollow support structures. The polyDES were highly transparent (transparency 95.6%), and the printed structures could be twisted, stretched, and compressed.

These authors also demonstrated the benefits of micro-structuring polyDES for enhancing the sensitivity of pressure sensors (Fig. 9(A)).<sup>102</sup> Specifically, AA:ChCl PDES formulation was used to fabricate submicrometer-scale protrusion structures (18 µm height and width) (Fig. 9(A), bottom left) that can maximize the sensing surface area subjected to deformation, producing high relative resistance changes under the action of an external force and outstanding sensitivity (348.28 kPa<sup>-1</sup>). The structured polyDES was flexible (36% strain) and worked over a wide pressure range (0.6 Pa–2 MPa), allowing for detection from air leakage of a vacuum-drying oven (Fig. 9(A), bottom middle) to the human pulse (Fig. 9(A), bottom right).

Wang *et al.* also developed an attractive PDES formulation for digital light processing (DLP) 3D printing consisting of AA:ChCl mixture, PEGDA as the crosslinker, phenylbis(2,4,6-trimethylbenzoyl)phosphine oxide (PPO) as the photoinitiator, nanoclay additive to further improve the mechanical properties, and Sudan I, a light absorber to mediate the

polymerization and alleviate the local high-temperature effects, which is beneficial for achieving high-resolution 3D printing (Fig. 9(B)).<sup>103</sup> These polyDES, dubbed SCIE (solid-state conductive ionoelastomers), were printed in different morphologies: gyroid, octahedral, and cubic (Fig. 9(C)), and they were utilized to fabricate a pressure sensor by the fusion with a piezoresistive design. The authors demonstrated that with the increase of external pressure from 0 to 100 kPa, the resistance variation was around 90.9%, 68.7%, and 34.1% for gyroid, octahedral, and cubic morphologies, respectively (Fig. 9(D), left), revealing how the pressure sensor sensitivity could be modulated by polyDES structuring. This enhanced performance results from the architecture-induced large deformation response, which was significantly higher for the gyroid lattice (up to 50% strain) than that of the cubic one (around 2%). Moreover, due to the excellent elasticity and recovery ability, the gyroid-based pressure sensor displays stable piezoresistive performance even under high-frequency pressure stimulation (Fig. 9(D), right).

In another creative work, Chu *et al.* used carboxylate cellulose nanocrystals (C-CNC) as a bio-template for the *in situ* formation of stable polyaniline (PANI) in the AA:ChCl PDES dynamically cross-linked with Al<sup>3+</sup> via coordination with -COOH groups.<sup>104</sup> This formulation was processed by DLP 3D printing using diphenyl(2,4,6-trimethylbenzoyl)phosphine (TPO) as the photoinitiator. The polyDESs could be configured in different shapes with high fidelity, were mechanically strong with a tensile strength and toughness of 4.4 MPa and 13.33 MJ m<sup>-3</sup>, and were able to support a hanging load of 500 g without breaking. With a conductivity of  $5.87 \times 10^{-2}$  S m<sup>-1</sup>, these 3D-printed elastomers were utilized to fabricate multi-functional strain, humidity, and temperature sensors for real-time and reliable detection of human motions, respiration, and body temperature.

Wang *et al.* also explored a ternary PDES formulation based on AAm:ChCl:4-acryloylmorpholine (AcMo), at different mole ratios, as a photocurable resin for liquid-crystal display (LCD) printing (Fig. 10(A)).<sup>105</sup> Synergistic hydrogen bonding among numerous hydroxy, amino, carbonyl, and morpholinyl groups in the PDES (Fig. 10(A), right) generated 3D-printed pieces with mechanical rigidity, heat resistance, and self-healing properties. The self-healing ability of these polyDES was demonstrated by cutting a printed structure into two parts and then rejoining at 90 °C for 24 h under a 10% humidity condition. The healed structure could load a weight of 200 g, exhibiting a self-healing efficiency of 75.9% (Fig. 10(B), left). Moreover, these materials could be assembled for various complex structures; for example, a porous box was deconstructed into six single planes that were printed separately (Fig. 10(B), right). Interestingly, these polyDES could be hydrolyzed in water at 90 °C, enabling their utilization as sacrificial molds to fabricate sophisticated structures from materials that would otherwise not be printable (Fig. 10(C)). With this strategy, the authors manufactured a finger guard for motion sensing.

PDES formulations have also been used to manufacture conductive fibers using spinning techniques. For instance, He *et al.* prepared fibers of 1 mm in diameter by

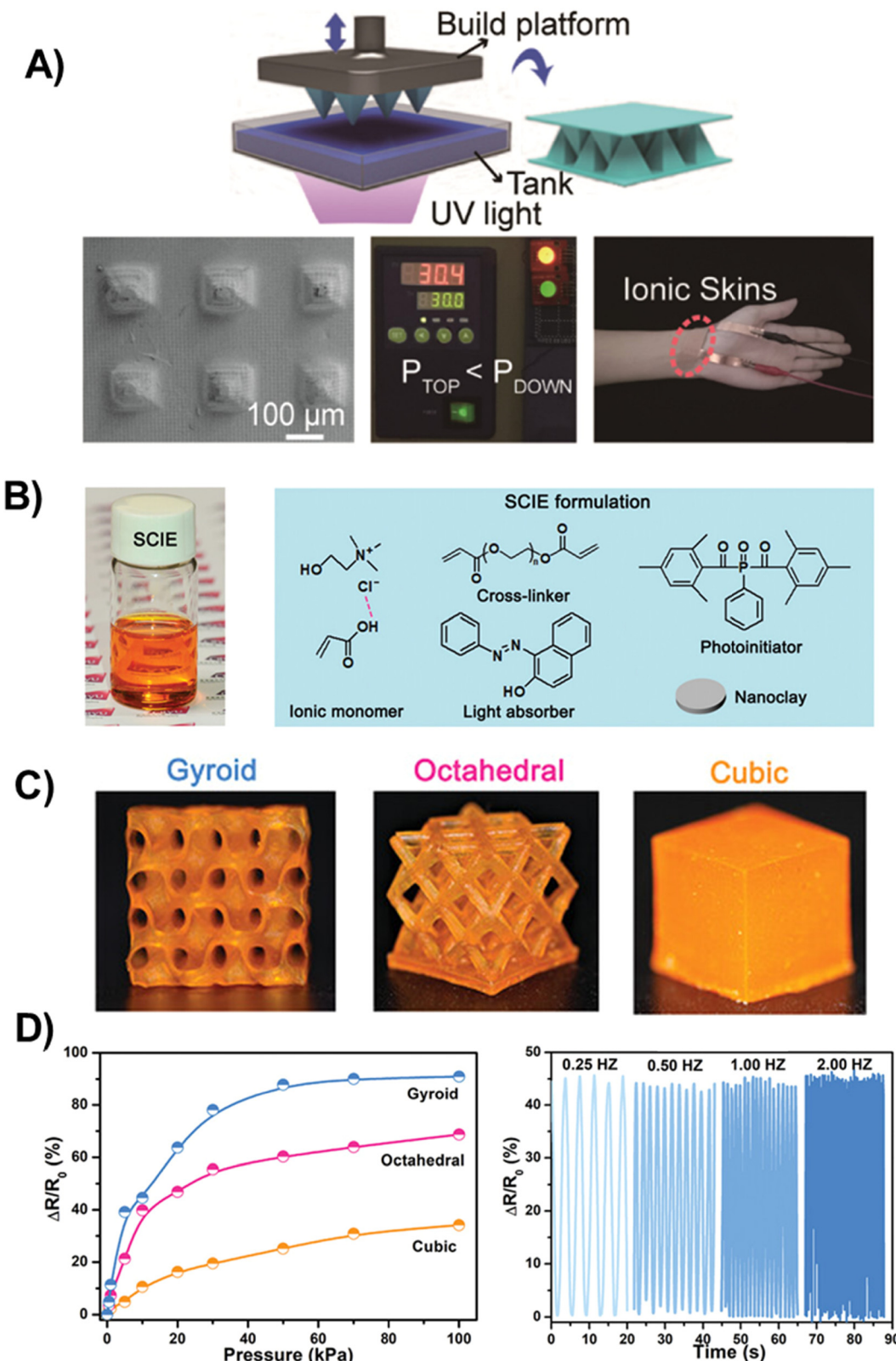


**Fig. 9** (A) Schematic diagram of the fabrication of the microstructured poly(AA/ChCl) sensor (top). Morphology of a pyramidal structured sensor containing submicrometric protrusions (bottom left). Monitoring of air leakage of a vacuum-drying oven using the microstructured poly(AA/ChCl) sensor (bottom middle). Optical images of polyDES structures as a sensor for pulse detection (bottom right). Adapted from ref. 102 with permission from the American Chemical Society. (B) Design of 3D-printable SCIE. Optical image of SCIE before photocuring (left). Molecular configuration of SCIE formulation containing PDES (AA:ChCl), nanofiller (nanoclay), crosslinker (PEGDA 700), light absorber (Sudan I), and photoinitiator (PPO). (C) Optical images of the printed SCIE-based structures (cubic, octahedral, and gyroid). (D) Piezoresistive performance of diverse printed SCIE-based sensors as a function of pressures (left). Piezoresistive performance of the printed gyroid-based piezoresistive sensor under different frequencies (right). Adapted from ref. 103 with permission from Wiley-VCH GmbH.

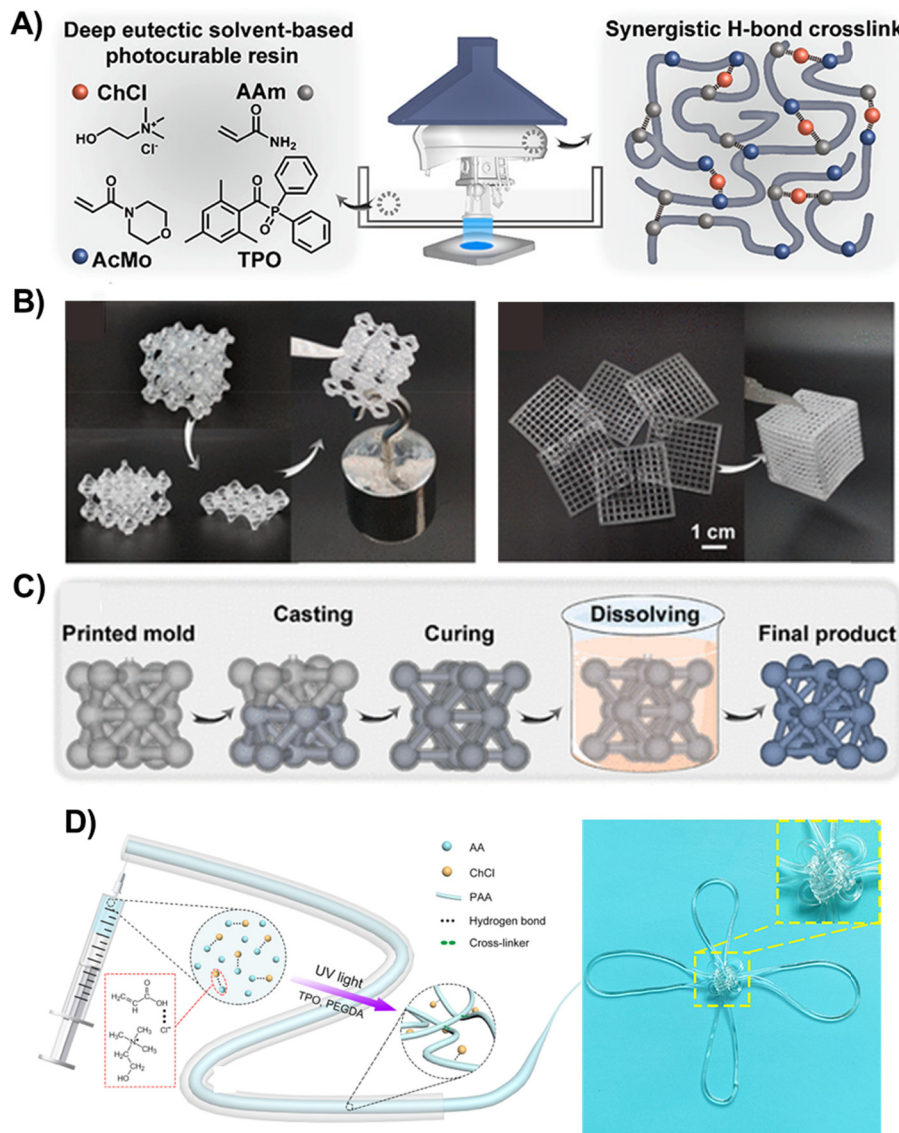


Fig. 10 (A) Schematic illustration of the composition of the polyDES and LCD printer for the fabrication of 3D objects (left) and the hydrogen-bonding network in the elastomers (right). (B) Photographs showing the self-healing capability of a 3D-printed lattice (left) and assembled 2D gridding to a 3D box structure (right). (C) Fabrication of 3D structures by sacrificing a 3D-printed mold. Adapted from ref. 105 with permission from the American Chemical Society. (D) Schematic illustration of the fabrication and properties of poly(AA:ChCl) fibers (left) and a digital image of a Chinese knot knitted from a polyDES fiber demonstrating its transparency and the ability to knit complex 3D structures (right). Adapted from ref. 106 with permission from the American Chemical Society.

photopolymerization of AA:ChCl cross-linked with PEGDA (polyDES  $T_g \approx -50$  °C), showing stable conductivity in an extremely low-humidity environment ( $\approx 2.5 \times 10^{-3}$  S m $^{-1}$ ), good elasticity at low and high temperatures (strains of 300% and 375% at  $-30$  °C and 100 °C, respectively), and resistance to organic solvents (Fig. 10(D)).<sup>106</sup> Furthermore, the fibers were highly transparent (average transmittance of  $>90\%$ ), and they could be knitted into complex 3D structures, such as a Chinese knot (Fig. 10(D), right).

Similarly, Huang *et al.* prepared Li $^{+}$ -doped poly(AA/ChCl) fibers (1 mm in diameter) *via* photopolymerization, although the term eutectogel was mistakenly assigned to these

materials.<sup>107</sup> Different lithium salts, including LiCl, LiBr, LiOAc, and LiTFSI, were used to toughen the polymer networks by forming dense interchain hydrogen-bond cross-links. The fibers' tensile strength, elongation, toughness, and ionic conductivity were 15 MPa, 300%, 38 MJ m $^{-3}$ , and  $\approx 6 \times 10^{-3}$  S m $^{-1}$ , respectively. Interestingly, the fibers showed shape-memory behavior and could be recycled and reprocessed by simply dissolving them in water at 60 °C and dry casting at 45 °C. As shape memory behavior was near the human body temperature, the authors postulated that these materials could be applied in wearable temperature monitoring and fever detection.

## 5. Final remarks and future perspectives

Ionic conductive elastomers based on PDES have a promising future in bioelectronics, as shown by their significant advances over the last two years. PolyDES are expected to demonstrate advances in several features, including cost-effectiveness, potential for tunable properties through variation of the solvent composition, and increased biocompatibility and biodegradability compared to classical poly(ionic liquids). However, to fully exploit the potential of polyDES materials, scientists should address several key points in the future. For instance, although the term PDES has been broadly adopted, the solid-liquid equilibrium phase diagram of the most used eutectic mixtures is not considered in the majority of the cases (even in the archetypical AA:ChCl mixture), overlooking the existence of negative deviations and the “deep” nature of the solvents. The lack of thermodynamic diagrams could be associated with the fact that many PDES show a  $T_g$  instead of a melting point in a broad composition range, as discussed here. In this particular scenario, the term low-transition-temperature mixtures (LTTMs) may be more appropriate for these reactive mixtures.

One of the main challenges for polyDES is enhancing their ionic conductivity while maintaining robust mechanical properties. It is not a trivial task, but it is necessary to optimize the performance of bioelectronic devices and fully exploit the advantages of these dry ionic conductors compared to gel-like materials.

On the other hand, we identify an urgent need to understand better the importance of ionic interactions *vs.* hydrogen bonding interactions. PolyDES are complex polymers where ionic and hydrogen bonding interactions affect different material properties such as  $T_g$ , mechanical, or transport properties, which are poorly understood. Similarly, the molecular weight of these ionic polymers has been rarely reported, and therefore, its impact on elastomeric behavior has not been appropriately addressed. In addition, considering that most applications in bioelectronics imply intimate contact of the polyDES with the skin or implantation into the body, their biosafety should be one relevant feature to be evaluated, although cytotoxicity is often dismissed.

One opportunity is its versatility in preparing new functional PDES, and the big panorama presented in this review is expected to help material scientists advance in this direction. For instance, it could be noticed that mixed ionic-electronic conducting polyDES has rarely been designed so far, except for some cases where polydopamine or polyaniline was incorporated. In the same direction, we also realize that polyDES elastomers were mainly intended for sensors, overlooking the fabrication of bioelectrodes for body signal recording, such as electrocardiography (ECG) or electromyography (EMG).

Finally, we hope this review allows us to broaden the perspective of material scientists on polyDES, potentially revealing aspects they may not have previously been considered. Introducing novel insights and innovative concepts seeks to

pave the way for exciting new avenues in their future applications.

## Data availability

No primary research results, software or code have been included and no new data were generated or analysed as part of this review.

## Conflicts of interest

The authors declare no conflict of interest.

## Acknowledgements

MLP has received funding from the European Union's Horizon 2020 research and innovation program under the Marie Skłodowska-Curie grant agreement no. 101028881. RJM is thankful for the financial support received from ANPCyT (PICT 2019-01265). JDMM acknowledges the financial support from PAPIIT-UNAM project IN115624. DM gratefully acknowledges the financial support from the Marie Skłodowska-Curie Research and Innovation Staff Exchanges program under grant agreement IONBIKE 2.0 MSCA-SE 101129945.

## References

- 1 D. Gao, K. Parida and P. S. Lee, Emerging Soft Conductors for Bioelectronic Interfaces, *Adv. Funct. Mater.*, 2020, **30**, 1907184.
- 2 Y. Fang, L. Meng, A. Prominski, E. N. Schaumann, M. Seebald and B. Tian, Recent advances in bioelectronics chemistry, *Chem. Soc. Rev.*, 2020, **49**, 7978–8035.
- 3 G. Balakrishnan, J. Song, C. Mou and C. J. Bettinger, Recent Progress in Materials Chemistry to Advance Flexible Bioelectronics in Medicine, *Adv. Mater.*, 2022, **34**, 2106787.
- 4 R. Shao, R. Ma, X. An, C. Wang and S. Sun, Challenges and emerging opportunities in transistor-based ultrathin electronics: design and fabrication for healthcare applications, *J. Mater. Chem. C*, 2022, **10**, 2450–2474.
- 5 Y. Fang, X. Li and Y. Fang, Organic bioelectronics for neural interfaces, *J. Mater. Chem. C*, 2015, **3**, 6424–6430.
- 6 B. Zhang, R. Xie, J. Jiang, S. Hao, B. Fang, J. Zhang, H. Bai, B. Peng, L. Li, Z. Liu and L. Fu, Implantable neural electrodes: from preparation optimization to application, *J. Mater. Chem. C*, 2023, **11**, 6550–6572.
- 7 J. H. Koo, J. K. Song, D. H. Kim and D. Son, Soft Implantable Bioelectronics, *ACS Mater. Lett.*, 2021, **3**, 1528–1540.
- 8 S. H. Sunwoo, K. H. Ha, S. Lee, N. Lu and D. H. Kim, Wearable and Implantable Soft Bioelectronics: Device Designs and Material Strategies, *Annu. Rev. Chem. Biomol. Eng.*, 2021, **12**, 359–391.

9 M. Jia and M. Rolandi, Soft and Ion-Conducting Materials in Bioelectronics: From Conducting Polymers to Hydrogels, *Adv. Healthcare Mater.*, 2020, **9**, 1901372.

10 S. Gong, Y. Lu, J. Yin, A. Levin and W. Cheng, Materials-Driven Soft Wearable Bioelectronics for Connected Healthcare, *Chem. Rev.*, 2024, **124**, 455–553.

11 Z. Zhang, Z. Zhu, P. Zhou, Y. Zou, J. Yang, H. Haick and Y. Wang, Soft Bioelectronics for Therapeutics, *ACS Nano*, 2023, **17**, 17634–17667.

12 X. Zhang, X. Chen, Z. Ye, W. Liu, X. Liu and X. Wang, Conductive hydrogels for bioelectronics: molecular structures, design principles, and operation mechanisms, *J. Mater. Chem. C*, 2023, **11**, 10785–10808.

13 R. Yang, X. Chen, Y. Zheng, K. Chen, W. Zeng and X. Wu, Recent advances in the 3D printing of electrically conductive hydrogels for flexible electronics, *J. Mater. Chem. C*, 2022, **10**, 5380–5399.

14 F. Fu, J. Wang, H. Zeng and J. Yu, Functional Conductive Hydrogels for Bioelectronics, *ACS Mater. Lett.*, 2020, **2**, 1287–1301.

15 Z. Li, J. Lu, T. Ji, Y. Xue, L. Zhao, K. Zhao, B. Jia, B. Wang, J. Wang, S. Zhang and Z. Jiang, Self-Healing Hydrogel Bioelectronics, *Adv. Mater.*, 2024, 2306350.

16 H. Yuk, B. Lu and X. Zhao, Hydrogel bioelectronics, *Chem. Soc. Rev.*, 2019, **48**, 1642–1667.

17 S. Inal, J. Rivnay, A. O. Suiu, G. G. Malliaras and I. McCulloch, Conjugated Polymers in Bioelectronics, *Acc. Chem. Res.*, 2018, **51**, 1368–1376.

18 M. Wang, P. Baek, A. Akbarinejad, D. Barker and J. Travas-Sejdic, Conjugated polymers and composites for stretchable organic electronics, *J. Mater. Chem. C*, 2019, **7**, 5534–5552.

19 F. Fu, J. Wang and J. Yu, Interpenetrating PAA-PEDOT conductive hydrogels for flexible skin sensors, *J. Mater. Chem. C*, 2021, **9**, 11794–11800.

20 R. D. Pyarasani, T. Jayaramudu and A. John, Polyaniline-based conducting hydrogels, *J. Mater. Sci.*, 2019, **54**, 974–996.

21 U. Riaz, N. Singh, F. Rashnas Srambikal and S. Fatima, A review on synthesis and applications of polyaniline and polypyrrole hydrogels, *Polym. Bull.*, 2023, **80**, 1085–1116.

22 P. W. Chen, D. H. Ji, Y. S. Zhang, C. Lee and M. Y. Yeh, Electroactive and Stretchable Hydrogels of 3,4-Ethylenedioxythiophene/thiophene Copolymers, *ACS Omega*, 2023, **8**, 6753–6761.

23 M. Shin, J. Lim, J. An, J. Yoon and J. W. Choi, Nanomaterial-based biohybrid hydrogel in bioelectronics, *Nano Convergence*, 2023, **10**, 8.

24 G. H. Lee, H. Woo, C. Yoon, C. Yang, J. Y. Bae, W. Kim, D. H. Lee, H. Kang, S. Han, S. K. Kang, S. Park, H. R. Kim, J. W. Jeong and S. Park, A Personalized Electronic Tattoo for Healthcare Realized by On-the-Spot Assembly of an Intrinsically Conductive and Durable Liquid-Metal Composite, *Adv. Mater.*, 2022, **34**, 2204159.

25 Y. Z. Zhang, J. K. El-Demellawi, Q. Jiang, G. Ge, H. Liang, K. Lee, X. Dong and H. N. Alshareef, MXene hydrogels: fundamentals and applications, *Chem. Soc. Rev.*, 2020, **49**, 7229–7251.

26 M. L. Picchio, A. Gallastegui, N. Casado, N. Lopez-Larrea, B. Marchiori, I. del Agua, M. Criado-Gonzalez, D. Mantione, R. J. Minari and D. Mecerreyes, Mixed Ionic and Electronic Conducting Eutectogels for 3D-Printable Wearable Sensors and Bioelectrodes, *Adv. Mater. Technol.*, 2022, **7**, 2101680.

27 G. C. Luque, M. L. Picchio, A. P. S. Martins, A. Dominguez-Alfaro, N. Ramos, I. del Agua, B. Marchiori, D. Mecerreyes, R. J. Minari and L. C. Tomé, 3D Printable and Biocompatible Iongels for Body Sensor Applications, *Adv. Electron. Mater.*, 2021, **7**, 2100178.

28 B. Yiming, Y. Han, Z. Han, X. Zhang, Y. Li, W. Lian, M. Zhang, J. Yin, T. Sun, Z. Wu, T. Li, J. Fu, Z. Jia and S. Qu, A Mechanically Robust and Versatile Liquid-Free Ionic Conductive Elastomer, *Adv. Mater.*, 2021, **33**, 2006111.

29 M. Isik, T. Lonjaret, H. Sardon, R. Marcilla, T. Herve, G. G. Malliaras, E. Ismailova and D. Mecerreyes, Cholinium-based ion gels as solid electrolytes for long-term cutaneous electrophysiology, *J. Mater. Chem. C*, 2015, **3**, 8942–8948.

30 N. Casado, S. Zendegi, L. C. Tomé, S. Velasco-Bosom, A. Aguzin, M. Picchio, M. Criado-Gonzalez, G. G. Malliaras, M. Forsyth and D. Mecerreyes, Injectable PEDOT:PSS/cholinium ionic liquid mixed conducting materials for electrocardiogram recordings, *J. Mater. Chem. C*, 2022, **10**, 15186–15193.

31 Z. Chen, N. Gao, Y. Chu, Y. He and Y. Wang, Ionic Network Based on Dynamic Ionic Liquids for Electronic Tattoo Application, *ACS Appl. Mater. Interfaces*, 2021, **13**, 33557–33565.

32 G. Jiang, G. Wang, Y. Zhu, W. Cheng, K. Cao, G. Xu, D. Zhao and H. Yu, A Scalable Bacterial Cellulose Ionogel for Multisensory Electronic Skin, *Research*, 2022, **2022**, 9814767.

33 J. Sun, R. Li, G. Lu, Y. Yuan, X. Zhu and J. Nie, A facile strategy for fabricating multifunctional ionogel based electronic skin, *J. Mater. Chem. C*, 2020, **8**, 8368–8373.

34 W. Li, K. Lin, L. Chen, D. Yang, Q. Ge and Z. Wang, Self-Powered Wireless Flexible Ionogel Wearable Devices, *ACS Appl. Mater. Interfaces*, 2023, **15**, 14768–14776.

35 Z. Yu and P. Wu, Water-Resistant Ionogel Electrode with Tailorable Mechanical Properties for Aquatic Ambulatory Physiological Signal Monitoring, *Adv. Funct. Mater.*, 2021, **31**, 2107226.

36 H. H. Chouhdry, D. H. Lee, A. Bag and N. E. Lee, A flexible artificial chemosensory neuronal synapse based on chemoreceptive ionogel-gated electrochemical transistor, *Nat. Commun.*, 2023, **14**, 821.

37 Y. Zhong, P. D. Nayak, S. Wustoni, J. Surgailis, J. Z. Parrado Agudelo, A. Marks, I. McCulloch and S. Inal, Ionic Liquid Gated Organic Electrochemical Transistors with Broadened Bandwidth, *ACS Appl. Mater. Interfaces*, 2023, DOI: [10.1021/acsami.3c11214](https://doi.org/10.1021/acsami.3c11214).

38 L. C. Tomé, L. Porcarelli, J. E. Bara, M. Forsyth and D. Mecerreyes, Emerging iongel materials towards applications in energy and bioelectronics, *Mater. Horiz.*, 2021, **8**, 3239–3265.

39 V. Patel, E. Das, A. Bhargava, S. Deshmukh, A. Modi and R. Srivastava, Ionogels for flexible conductive substrates and their application in biosensing, *Int. J. Biol. Macromol.*, 2024, **254**, 127736.

40 C. C. Yan, W. Li, Z. Liu, S. Zheng, Y. Hu, Y. Zhou, J. Guo, X. Ou, Q. Li, J. Yu, L. Li, M. Yang, Q. Liu and F. Yan, Ionogels: Preparation, Properties and Applications, *Adv. Funct. Mater.*, 2024, 2314408.

41 L. C. Tomé and D. Mecerreyes, Emerging Ionic Soft Materials Based on Deep Eutectic Solvents, *J. Phys. Chem. B*, 2020, **124**, 8465–8478.

42 J. D. Mota-Morales and E. Morales-Narváez, Transforming nature into the next generation of bio-based flexible devices: New avenues using deep eutectic systems, *Matter*, 2021, **4**, 2141–2162.

43 C. Luo, Z. Huang, Z. H. Guo and K. Yue, Recent Progresses in Liquid-Free Soft Ionic Conductive Elastomers, *Chin. J. Chem.*, 2023, **41**, 835–860.

44 F. Guthrie, On eutexia, London, Edinburgh, *Dublin Philos. Mag. J. Sci.*, 1884, **17**, 462–482, DOI: [10.1080/14786448408627543](https://doi.org/10.1080/14786448408627543).

45 M. A. R. Martins, S. P. Pinho and J. A. P. Coutinho, Insights into the Nature of Eutectic and Deep Eutectic Mixtures, *J. Solution Chem.*, 2018, **48**, 962–982.

46 A. P. Abbott, G. Capper, D. L. Davies, R. K. Rasheed and V. Tambyrajah, Novel solvent properties of choline chloride/urea mixtures, *Chem. Commun.*, 2003, 70–71.

47 D. O. Abrantes and J. A. P. Coutinho, Everything You Wanted to Know about Deep Eutectic Solvents but Were Afraid to Be Told, *Annu. Rev. Chem. Biomol. Eng.*, 2023, **14**, 141–163.

48 A. van den Bruinhorst and M. Costa Gomes, Is there depth to eutectic solvents?, *Curr. Opin. Green Sustainable Chem.*, 2022, **37**, 100659.

49 M. Francisco, A. Van Den Bruinhorst and M. C. Kroon, Low-Transition-Temperature Mixtures (LTTMs): A New Generation of Designer Solvents, *Angew. Chem., Int. Ed.*, 2013, **52**, 3074–3085.

50 Y. Tanaka, K. Ajino, H. Ogawa and H. Mori, Design of metal salt/amide-based deep eutectic monomers toward sustainable production of ion-conductive polymers by radical polymerization, *Mater. Today Chem.*, 2022, **26**, 101033.

51 M. Isik, F. Ruiperez, H. Sardon, A. Gonzalez, S. Zulfiqar and D. Mecerreyes, Innovative Poly(Ionic Liquid)s by the Polymerization of Deep Eutectic Monomers, *Macromol. Rapid Commun.*, 2016, **37**, 1135–1142.

52 S. Wierzbicki, K. Mielczarek, M. Topa-Skwarczyńska, K. Mokrzyński, J. Ortyl and S. Bednarz, Visible light-induced photopolymerization of Deep Eutectic Monomers, based on methacrylic acid and tetrabutylammonium salts with different anion structures, *Eur. Polym. J.*, 2021, **161**, 110836.

53 K. Mielczarek, S. Wierzbicki, M. Topa-Skwarczyńska, S. Bujok, R. Konefal, M. Nevoralová, J. Ortyl, H. Beneš and S. Bednarz, Polymerization of renewable itaconic acid in deep eutectic monomers: Effect of the quaternary ammonium cation structure, *Eur. Polym. J.*, 2024, **203**, 112677.

54 J. D. Mota-Morales, R. J. Sánchez-Leija, A. Carranza, J. A. Pojman, F. del Monte and G. Luna-Bárcenas, Free-radical polymerizations of and in deep eutectic solvents: Green synthesis of functional materials, *Prog. Polym. Sci.*, 2018, **78**, 139–153.

55 S. Li, Y. Jiang, Y. Zhu, J. Fu and S. Yan, Facile preparation of stretchable and multifunctional ionic gels via frontal polymerization of polymerizable ternary deep eutectic monomers with a long pot life, *Colloid Polym. Sci.*, 2022, **301**, 19–29.

56 J. D. Mota-Morales, M. C. Gutiérrez, I. C. Sanchez, G. Luna-Bárcenas and F. Del Monte, Frontal polymerizations carried out in deep-eutectic mixtures providing both the monomers and the polymerization medium, *Chem. Commun.*, 2011, **47**, 5328–5330.

57 J. D. Mota-Morales, M. C. Gutiérrez, M. L. Ferrer, I. C. Sanchez, E. A. Elizalde-Peña, J. A. Pojman, F. Del Monte and G. Luna-Bárcenas, Deep eutectic solvents as both active fillers and monomers for frontal polymerization, *J. Polym. Sci., Part A: Polym. Chem.*, 2013, **51**, 1767–1773.

58 L. Lin, R. Li, G. Chen, X. Wang, J. Cheng, J. Zhao, K. Zhao and M. He, Impact of hydrogen bonding interaction energy on the polymerization kinetics of polymerizable deep eutectic solvent monomers, *Polym. Chem.*, 2024, **15**, 783–795.

59 M. Isik, S. Zulfiqar, F. Edhaim, F. Ruiperez, A. Rothenberger and D. Mecerreyes, *ACS Sustainable Chem. Eng.*, 2016, **4**, 7200–7208.

60 K. Ajino, A. Torii, H. Ogawa and H. Mori, Synthesis of ion-conductive polymers by radical polymerization of deep eutectic monomers bearing quaternary ammonium groups with urea, *Polymer*, 2020, **204**, 122803.

61 J. L. de Lacalle, A. Gallastegui, J. L. Olmedo-Martínez, M. Moya, N. Lopez-Larrea, M. L. Picchio and D. Mecerreyes, Multifunctional Ionic Polymers from Deep Eutectic Monomers Based on Polyphenols, *ACS Macro Lett.*, 2023, **12**, 125–132.

62 G. Zhu, J. Zhang, J. Huang, X. Yu, J. Cheng, Q. Shang, Y. Hu, C. Liu, M. Zhang, L. Hu and Y. Zhou, Self-Healing, Antibacterial, and 3D-Printable Polymerizable Deep Eutectic Solvents Derived from Tannic Acid, *ACS Sustainable Chem. Eng.*, 2022, **10**, 7954–7964.

63 Y. Nahar, J. Horne, V. Truong, A. C. Bissember and S. C. Thickett, Preparation of thermoresponsive hydrogels via polymerizable deep eutectic monomer solvents, *Polym. Chem.*, 2021, **12**, 254–264.

64 P. Qi, S. Yuan, Y. Liu, R. Dong, A. Song and J. Hao, Unexpected Polymerization-Induced Luminescence in Deep Eutectic Solvent (DES)-Based Polym., *Adv. Opt. Mater.*, 2023, **11**, 2300861.

65 X. Qu, W. Niu, R. Wang, Z. Li, Y. Guo, X. Liu and J. Sun, Solid-state and liquid-free elastomeric ionic conductors with autonomous self-healing ability, *Mater. Horiz.*, 2020, **7**, 2994–3004.

66 L. Shi, T. Zhu, G. Gao, X. Zhang, W. Wei, W. Liu and S. Ding, Highly stretchable and transparent ionic conducting elastomers, *Nat. Commun.*, 2018, **9**, 2630.

67 R. Li, G. Chen, M. He, J. Tian and B. Su, Patternable transparent and conductive elastomers towards flexible tactile/strain sensors, *J. Mater. Chem. C*, 2017, **5**, 8475–8481.

68 L. Ren'Ai, K. Zhang, G. Chen, B. Su, J. Tian, M. He and F. Lu, Green polymerizable deep eutectic solvent (PDES) type conductive paper for origami 3D circuits, *Chem. Commun.*, 2018, **54**, 2304–2307.

69 M. Wang, R. Li, G. Chen, S. Zhou, X. Feng, Y. Chen, M. He, D. Liu, T. Song and H. Qi, Highly Stretchable, Transparent, and Conductive Wood Fabricated by in Situ Photopolymerization with Polymerizable Deep Eutectic Solvents, *ACS Appl. Mater. Interfaces*, 2019, **11**, 14313–14321.

70 K. Zhang, G. Chen, R. Li, K. Zhao, J. Shen, J. Tian and M. He, Facile Preparation of Highly Transparent Conducting Nanopaper with Electrical Robustness, *ACS Sustainable Chem. Eng.*, 2020, **8**, 5132–5139.

71 R. Li, T. Fan, G. Chen, H. Xie, B. Su and M. He, Highly transparent, self-healing conductive elastomers enabled by synergistic hydrogen bonding interactions, *Chem. Eng. J.*, 2020, **393**, 124685.

72 K. Zhang, R. Li, G. Chen, J. Yang, J. Tian and M. He, Polymerizable deep eutectic solvent-based mechanically strong and ultra-stretchable conductive elastomers for detecting human motions, *J. Mater. Chem. A*, 2021, **9**, 4890–4897.

73 Q. Zhang, G. Chen, R. Li, L. Lin and M. He, Mechanically tough yet self-healing transparent conductive elastomers obtained using a synergic dual cross-linking strategy, *Polym. Chem.*, 2021, **12**, 2016–2023.

74 R. Li, T. Fan, G. Chen, K. Zhang, B. Su, J. Tian and M. He, Autonomous Self-Healing, Antifreezing, and Transparent Conductive Elastomers, *Chem. Mater.*, 2020, **32**, 874–881.

75 R. Li, G. Chen, T. Fan, K. Zhang and M. He, Transparent conductive elastomers with excellent autonomous self-healing capability in harsh organic solvent environments, *J. Mater. Chem. A*, 2020, **8**, 5056–5061.

76 P. Sang, R. Li, K. Zhang, G. Chen, K. Zhao and M. He, Liquid-Free Ionic Conductive Elastomers with High Mechanical Strength and Rapid Healable Ability, *ACS Appl. Polym. Mater.*, 2022, **4**, 3543–3551.

77 W. Xia, Y. Yu, C. Zhou, W. Wang, Z. Wu and H. Chen, Itaconic acid-enhanced robust ionic conductive elastomers for strain/pressure sensors, *J. Mater. Chem. C*, 2023, **11**, 16545–16553.

78 Y. Jin, J. Li, M. Zhang, J. He and P. Ni, Unexpected mechanically robust ionic conductive elastomer constructed from an itaconic acid-involved polymerizable DES, *Chem. Commun.*, 2023, **59**, 12998–13001.

79 D. Du, J. Zhou, D. Shi, W. Dong and M. Chen, Cross-Linked, Transient Ionic Conductive Elastomer with Extreme Stretchability, Healability, and Degradability for Detecting Human Motions, *ACS Appl. Polym. Mater.*, 2022, **4**, 4972–4979.

80 D. Zhang, X. Li, J. Li, Q. Wang, X. Dong, Y. Wu, Z. Li, X. Xie, Z. Liu, F. Xiu, W. Huang and J. Liu, Phase-Segregated Ductile Eutectogels with Ultrahigh Modulus and Toughness for Antidamaging Fabric Perception, *Small*, 2023, 2306557.

81 M. Wang, R. Li, X. Feng, C. Dang, F. Dai, X. Yin, M. He, D. Liu and H. Qi, Cellulose Nanofiber-Reinforced Ionic Conductors for Multifunctional Sensors and Devices, *ACS Appl. Mater. Interfaces*, 2020, **12**, 27545–27554.

82 X. Sun, Y. Zhu, J. Zhu, K. Le, P. Servati and F. Jiang, Tough and Ultrastretchable Liquid-Free Ion Conductor Strengthened by Deep Eutectic Solvent Hydrolyzed Cellulose Microfibers, *Adv. Funct. Mater.*, 2022, **32**, 2202533.

83 X. Li, J. Liu, Q. Guo, X. Zhang and M. Tian, Polymerizable Deep Eutectic Solvent-Based Skin-Like Elastomers with Dynamic Schemochrome and Self-Healing Ability, *Small*, 2022, **18**, 2201012.

84 M. Wang, Z. Lai, X. Jin, T. Sun, H. Liu and H. Qi, Multi-functional Liquid-Free Ionic Conductive Elastomer Fabricated by Liquid Metal Induced Polymerization, *Adv. Funct. Mater.*, 2021, **31**, 2101957.

85 X. Zhang, Q. Fu, Y. Wang, H. Zhao, S. Hao, C. Ma, F. Xu and J. Yang, Tough Liquid-Free Ionic Conductive Elastomers with Robust Adhesion and Self-Healing Properties for Ionotronic Devices, *Adv. Funct. Mater.*, 2024, **34**, 2307400.

86 X. Sun, Y. Zhu, Z. Yu, Y. Liang, J. Zhu and F. Jiang, Dialcohol Cellulose Nanocrystals Enhanced Polymerizable Deep Eutectic Solvent-Based Self-Healing Ion Conductors with Ultra-Stretchability and Sensitivity, *Adv. Sens. Res.*, 2023, **2**, 2200045.

87 C. Lu, X. Wang, Y. Shen, C. Wang, J. Wang, Q. Yong and F. Chu, Liquid-Free, Anti-Freezing, Solvent-Resistant, Cellulose-Derived Ionic Conductive Elastomer for Stretchable Wearable Electronics and Triboelectric Nanogenerators, *Adv. Funct. Mater.*, 2022, **32**, 2207714.

88 N. Wang, X. Yang and X. Zhang, Ultrarobust subzero healable materials enabled by polyphenol nano-assemblies, *Nat. Commun.*, 2023, **14**, 814.

89 Q. Chen, H. Chen, L. Zhu and J. Zheng, Fundamentals of double network hydrogels, *J. Mater. Chem. B*, 2015, **3**, 3654–3676.

90 H. Xin, Double-Network Tough Hydrogels: A Brief Review on Achievements and Challenges, *Gels*, 2022, **8**, 247.

91 K. Zhao, K. Zhang, R. Li, P. Sang, H. Hu and M. He, A very mechanically strong and stretchable liquid-free double-network ionic conductor, *J. Mater. Chem. A*, 2021, **9**, 23714–23721.

92 Z. Hua, G. Chen, K. Zhao, R. Li and M. He, A Repeatable Self-Adhesive Liquid-Free Double-Network Ionic Conductor with Tunable Multifunctionality, *ACS Appl. Mater. Interfaces*, 2022, **14**, 22418–22425.

93 Y. Han, K. Zhao, G. Chen, R. Li, C. Zhou, Z. Hua, H. Duan and M. He, A mechanically strong and self-adhesive all-solid-state ionic conductor based on the double-network strategy, *J. Mater. Chem. A*, 2023, **11**, 19637–19644.

94 C. Lu, C. Wang, J. Wang, Q. Yong and F. Chu, Integration of hydrogen bonding interaction and Schiff-base chemistry toward self-healing, anti-freezing, and conductive elastomer, *Chem. Eng. J.*, 2021, **45**, 130652.

95 N. Tang, Y. Jiang, K. Wei, Z. Zheng, H. Zhang and J. Hu, Evolutionary Reinforcement of Polymer Networks: A Stepwise-Enhanced Strategy for Ultrarobust Eutectogels, *Adv. Mater.*, 2024, **36**, 2309576.

96 K. Zhang, R. Li, G. Chen, X. Wang and M. He, Self-Adhesive Dry Ionic Conductors Based on Supramolecular Deep Eutectic Polymers, *Chem. Mater.*, 2022, **34**, 3736–3743.

97 H. Cheng, K. Yang, Y. Zhang, S. Liao, M. Du, J. Li, N. Ma, M. Xue, X. Zhang and Y. Wang, A Novel Ionic Conductive Polyurethane Based on Deep Eutectic Solvent Continuing Traditional Merits, *ACS Appl. Mater. Interfaces*, 2022, **14**, 52402–52410.

98 P. Yao, Q. Bao, Y. Yao, M. Xiao, Z. Xu, J. Yang and W. Liu, Environmentally Stable, Robust, Adhesive, and Conductive Supramolecular Deep Eutectic Gels as Ultrasensitive Flexible Temperature Sensor, *Adv. Mater.*, 2023, **35**, 2300114.

99 W. Chen, W. Sun, J. Li, Y. Qiu, L. Qiu, J. Ma, N. Li and X. Ji, Multifunctional Conductive Elastomers Based on Tannic Acid and Polymerizable 1-Butyl-3-methylimidazolium Chloride/Acrylic Acid Deep Eutectic Solvent, *ACS Appl. Polym. Mater.*, 2024, **6**, 180–191.

100 N. Li, Y. Qiu, J. Ma, L. Qiu, W. Sun, J. Li, Z. Han, W. Chen and X. Ji, Mechanically Robust and Multifunctional Ionogels Based on Cellulose and Polymerizable 1-Butyl-3-Methylimidazolium Chloride/Acrylamide Deep Eutectic Solvent, *ACS Appl. Polym. Mater.*, 2023, **5**, 9974–9986.

101 L. Cai, G. Chen, B. Su and M. He, 3D printing of ultra-tough, self-healing transparent conductive elastomeric sensors, *Chem. Eng. J.*, 2021, **426**, 130545.

102 L. Cai, G. Chen, J. Tian, B. Su and M. He, Three-dimensional Printed Ultrahighly Sensitive Bioinspired Ionic Skin Based on Submicrometer-Scale Structures by Polymerization Shrinkage, *Chem. Mater.*, 2021, **33**, 2072–2079.

103 C. Zhang, H. Zheng, J. Sun, Y. Zhou, W. Xu, Y. Dai, J. Mo and Z. Wang, 3D Printed, Solid-State Conductive Ionoelastomer as a Generic Building Block for Tactile Applications, *Adv. Mater.*, 2022, **34**, 2105996.

104 C. Lu, X. Wang, Q. Jia, S. Xu, C. Wang, S. Du, J. Wang, Q. Yong and F. Chu, 3D printed mechanical robust cellulose derived liquid-free ionic conductive elastomer for multifunctional electronic devices, *Carbohydr. Polym.*, 2024, **324**, 121496.

105 Y. Li, R. K. Kankala, L. Wu, A. Z. Chen and S. Bin Wang, 3D-Printed Photocurable Resin with Synergistic Hydrogen Bonding Based on Deep Eutectic Solvent, *ACS Appl. Polym. Mater.*, 2023, **5**, 991–1001.

106 X. Wang, G. Chen, L. Cai, R. Li and M. He, Weavable Transparent Conductive Fibers with Harsh Environment Tolerance, *ACS Appl. Mater. Interfaces*, 2021, **13**, 8952–8959.

107 L. Fang, C. Zhang, W. Ge, M. Rong, F. Chen, Z. Chen, X. Wang, Z. Zheng and Q. Huang, Facile spinning of tough and conductive eutectogel fibers via  $\text{Li}^+$ -induced dense hydrogen-bond networks, *Chem. Eng. J.*, 2023, **478**, 147405.